Cell Reports

Article

Retinoic Acid Promotes Endothelial Cell Cycle Early G1 State to Enable Human Hemogenic Endothelial Cell Specification

Graphical Abstract

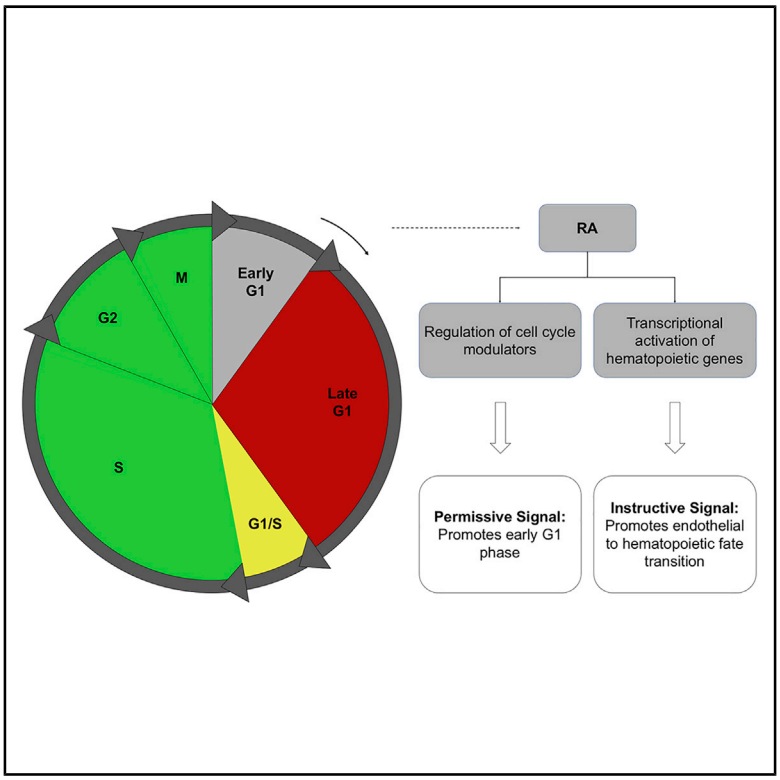

Authors

Jingyao Qiu, Sofia Nordling, Hema H. Vasavada, Eugene C. Butcher, Karen K. Hirschi

Correspondence

kkh4yy@virginia.edu

In Brief

Retinoic acid signaling and cell-cycle control are known to promote mouse hemogenic endothelial cell specification. Qiu et al. present a protocol to derive endothelial cells from human stem cells and promote their hemogenic specification. These insights provide guidance for generating human hemogenic endothelial cells for regenerative medicine applications.

Highlights

- A simple and efficient protocol to derive human hemogenic endothelial cells is described
- Functional human hemogenic endothelial cells are characterized on a clonal level
- Retinoic acid signaling is required for human hemogenic endothelial specification
- Cell-cycle state is a critical determinant of human endothelial cell specification

Qiu et al., 2020, Cell Reports *33*, 108465
December 1, 2020
https://doi.org/10.1016/j.celrep.2020.108465

CellPress

Cell Reports

CellPress
OPEN ACCESS

Article

Retinoic Acid Promotes Endothelial Cell Cycle Early G1 State to Enable Human Hemogenic Endothelial Cell Specification

Jingyao Qiu,[1,2,3,4,5] Sofia Nordling,[6] Hema H. Vasavada,[3] Eugene C. Butcher,[6,7,8] and Karen K. Hirschi[1,2,3,4,5,9,10,*]

[1]Department of Medicine, Yale University School of Medicine, New Haven, CT 06520, USA
[2]Department of Genetics, Yale University School of Medicine, New Haven, CT 06520, USA
[3]Yale Cardiovascular Research Center, Yale University School of Medicine, New Haven, CT 06520, USA
[4]Vascular Biology and Therapeutics Program, Yale University School of Medicine, New Haven, CT 06520, USA
[5]Yale Stem Cell Center, Yale University School of Medicine, New Haven, CT 06520, USA
[6]Laboratory of Immunology and Vascular Biology, Department of Pathology, Stanford University School of Medicine, Stanford, CA 94305, USA
[7]Palo Alto Veterans Institute for Research, VA Palo Alto Health Care System, Palo Alto, CA 94304, USA
[8]The Center for Molecular Biology and Medicine, VA Palo Alto Health Care System, Palo Alto, CA 94304, USA
[9]Department of Cell Biology, University of Virginia, Charlottesville, VA 22908, USA
[10]Lead Contact
*Correspondence: kkh4yy@virginia.edu
https://doi.org/10.1016/j.celrep.2020.108465

SUMMARY

Development of blood-forming (hemogenic) endothelial cells that give rise to hematopoietic stem and progenitor cells (HSPCs) is critical during embryogenesis to generate the embryonic and postnatal hematopoietic system. We previously demonstrated that the specification of murine hemogenic endothelial cells is promoted by retinoic acid (RA) signaling and requires downstream endothelial cell cycle control. Whether this mechanism is conserved in human hemogenic endothelial cell specification is unknown. Here, we present a protocol to derive primordial endothelial cells from human embryonic stem cells and promote their specification toward hemogenic endothelial cells. Furthermore, we demonstrate that RA treatment significantly increases human hemogenic endothelial cell specification. That is, RA promotes endothelial cell cycle arrest to enable RA-induced instructive signals to upregulate the genes needed for hematopoietic transition. These insights provide guidance for the *ex vivo* generation of autologous human hemogenic endothelial cells that are needed to produce human HSPCs for regenerative medicine applications.

INTRODUCTION

Mammalian hematopoiesis occurs in two phases during embryogenesis: primitive and definitive hematopoiesis. In the mouse, definitive hematopoiesis takes place mainly within the yolk sac and the aorta-gonad-mesonephros (AGM) region (de Bruijn et al., 2000; Medvinsky and Dzierzak, 1996; Müller et al., 1994), and is marked by the generation of multipotent hematopoietic stem and progenitor cells (HSPCs) from specialized blood-forming (or hemogenic) endothelial cells. Transplantation experiments have shown that cells isolated from the AGM region as early as embryonic day (E) 10.5 can confer long-term hematopoietic repopulation in lethally irradiated recipient mice (de Bruijn et al., 2000; Medvinsky and Dzierzak, 1996; Müller et al., 1994); these cells are referred to as adult repopulating HSPCs. Thus, the HSPCs produced by hemogenic endothelial cells are the foundation of the adult hematopoietic hierarchy, providing the continuous production of blood cells throughout life. Therefore, understanding the mechanisms by which human hemogenic endothelial cells are specified is a critical first step toward generating human HSPCs for the treatment of hematopoietic disorders.

Several regulators have been previously implicated in the specification of murine hemogenic endothelial cells in the yolk sac and AGM, including retinoic acid (RA), c-Kit, Notch, and p27 (Bohnsack et al., 2004; Chanda et al., 2013; Goldie et al., 2008; Lai et al., 2003; Marcelo et al., 2013b; Niederreither et al., 1999). It is believed that RA promotes a signaling cascade, mediating the downstream Kit-Notch-p27 signaling axis (reviewed in Marcelo et al., 2013a). p27 functions as a cyclin-dependent kinase (CDK) inhibitor that restricts cell cycle progression at G1 phase (Hitomi et al., 2006), and we (Marcelo et al. (2013b) have previously shown the necessity of p27-mediated cell cycle arrest in the process of murine hemogenic endothelial cell specification. In addition, a number of studies have demonstrated the link between the cell cycle state of stem cells and cell fate decisions (Gonzales et al., 2015; Pauklin and Vallier, 2013; Singh et al., 2013) and suggest that cells preferably make

cell fate decisions during G1 phase (Dekker, 2014; Tumbar and Belmont, 2001). Furthermore, there are molecular differences between early G1 and late G1 that provide distinct windows of opportunity for extrinsic signals to promote the differentiation of distinct phenotypes (Pauklin and Vallier, 2013). Whether hemogenic specification of endothelial cells occurs specifically in G1 phase and whether early versus late G1 state is more permissive for this process remain to be determined, as does the potential role of RA in the regulation of human hemogenic endothelial cell specification. We investigate these unanswered questions in this study.

Elucidating the mechanism(s) by which endothelial cells acquire blood-forming potential is a critical first step toward understanding the establishment of the hematopoietic system. Such studies provide insights into the production of cells that can ultimately generate human HSPCs *ex vivo* from potentially autologous human pluripotent stem cells, which can be used for the treatment of hematopoietic disorders. Toward this goal, we established an *in vitro* model of human hemogenic endothelial cell development that is feeder-free, requires few growth factors, and can be performed in 1 week. Thus, unlike other systems using feeder cells or embryoid bodies, our system minimizes potential confounding effects introduced by mouse cells or the concurrent development of other organ systems. This highly controlled culture environment allows us to dissect the regulation of human endothelial cell development and their hemogenic specification. Using this system, we discovered the essential roles of RA and the cell cycle state in the process of human hemogenic endothelial cell specification. We believe that this system will serve as a critical tool for further studying human hemogenic endothelial cell development, which is the first step toward optimizing the production of transplantable blood cells for therapeutic purposes.

RESULTS

Simple *In Vitro* System to Derive Human Hemogenic Endothelial Cells from Human Embryonic Stem Cells (hESCs)

A number of protocols were developed to differentiate hESCs toward hematopoietic cells (Krassowska et al., 2006; Lengerke et al., 2009; Niwa et al., 2011); however, these protocols require either usage of feeder cells, formation of embryoid bodies, and/or addition of numerous growth factors, and can take up to 3 weeks. Sriram et al. (2015) previously established a feeder-free protocol to differentiate hESC into endothelial cells. We discovered that treating hESC-derived endothelial cells with RA can promote specification toward hemogenic endothelial cells that give rise to differentiated hematopoietic lineages (Figure 1A). This protocol requires no feeder cells or formation of embryoid bodies. In addition, it requires only 4 growth factors and takes ~1 week from start to finish.

To validate the protocol, we performed qPCR analysis of markers associated with cell fate transitions (Figure 1B). We found that on day 1 (D1) of differentiation, the level of pluripotency marker SOX2 significantly decreased, accompanied by the upregulation of primitive streak marker TBXT. Primitive streak cells were then differentiated into mesoderm cells marked by elevated HAND1 expression on D3. Endothelial cell marker CDH5 peaked on D5, with elevated expression of both arterial endothelial cell marker EFNB2 and venous endothelial cell marker EPHB4. Upon treatment with 0.5 μM RA, we observed gradually increased expression of RUNX1 mRNA, which marks the transition toward hematopoietic cell fates.

We then performed flow cytometry on D8 to isolate adherent endothelial cells ($CD31^+CD45^-$) and blood cells ($CD45^+$), and confirmed their phenotypes on the protein level (Figure 1C). We also observed 40%–45% live cells in the culture supernatant (Figure S2A); using Giemsa staining to better evaluate their phenotype, we identified blood cells of all lineages, including erythrocytes, lymphocytes, macrophages, monocytes, megakaryocytes, neutrophils, and basophils (Figure 1D). Lastly, we confirmed the generation of blood cells of multiple lineages using flow cytometry, using markers of lymphoid cells (CD20 and CD3), myeloid cells (CD14, CD66b, CD41, and CD235ab), and leukocytes (CD11b and CD45) (Figures 1E, S1, and S2). These data demonstrate that our protocol promotes the efficient differentiation of hESCs into endothelial cells and hematopoietic cells.

Characterization of the Phenotype of Human Hemogenic Endothelial Cells on Population and Single-Cell Levels

We next sought to identify the subset of endothelial cells that presumably generated the hematopoietic cells, and define their phenotype. The phenotype of murine hemogenic endothelial cells has been previously defined as $Flk\text{-}1^+Kit^+CD45^-$Side Population (SP) cells (Goldie et al., 2008; Marcelo et al., 2013b; Nadin et al., 2003; Wulf et al., 2003). Here, we used flow cytometric separation of subpopulations of cells and a methylcellulose-based blood-forming assay to define the phenotype of human hemogenic endothelial cells as $CD31^+KDR^+KIT^+CD34^+CDH5^-CD45^-$ cells, as outlined in Figure 2A and described further below.

Initially, we tested the ability of our whole-cell population to generate multiple hematopoietic cell colony types, including multilineage CFU-GEMM (colony-forming unit-granulocyte/erythrocyte/monocyte/megakaryocyte), CFU-GM (colony-forming unit-granulocyte/monocyte), BFU-E (burst-forming unit-erythroid) and CFU-E (colony-forming unit-erythroid) colonies (Figure 2B). To begin to characterize the phenotype of the blood-forming endothelial cells within this population, we excluded other cells with blood-forming potential, specifically $CD45^+$ HSPCs, by isolating $CD45^-$ cells using fluorescence-activated cell sorting (FACS). We then further separated the $CD45^-$ cells into various subgroups, based on the expression of known endothelial- or hematopoietic-enriched cell surface proteins. Among the $CD45^-$ cells, hematopoietic potential was enriched within the $CD31^+$ population (Figures 2C and S3A).

We then isolated $CD31^+CD45^-$ cells, known to be an enriched population of endothelial cells, and similarly separated them into additional subgroups based on the expression of specific proteins enriched in endothelial or hematopoietic cells. Among the $CD31^+CD45^-$ endothelial cells, hematopoietic potential was enriched within the $CDH5^-$ and $CD34^-$ populations (Figures 2D and S3B). Since CD34 marks definitive human hematopoietic progenitors but not primitive hematopoietic progenitors (Dege and Sturgeon, 2017), we further isolated $CD31^+CD45^-CDH5^-$ cells.

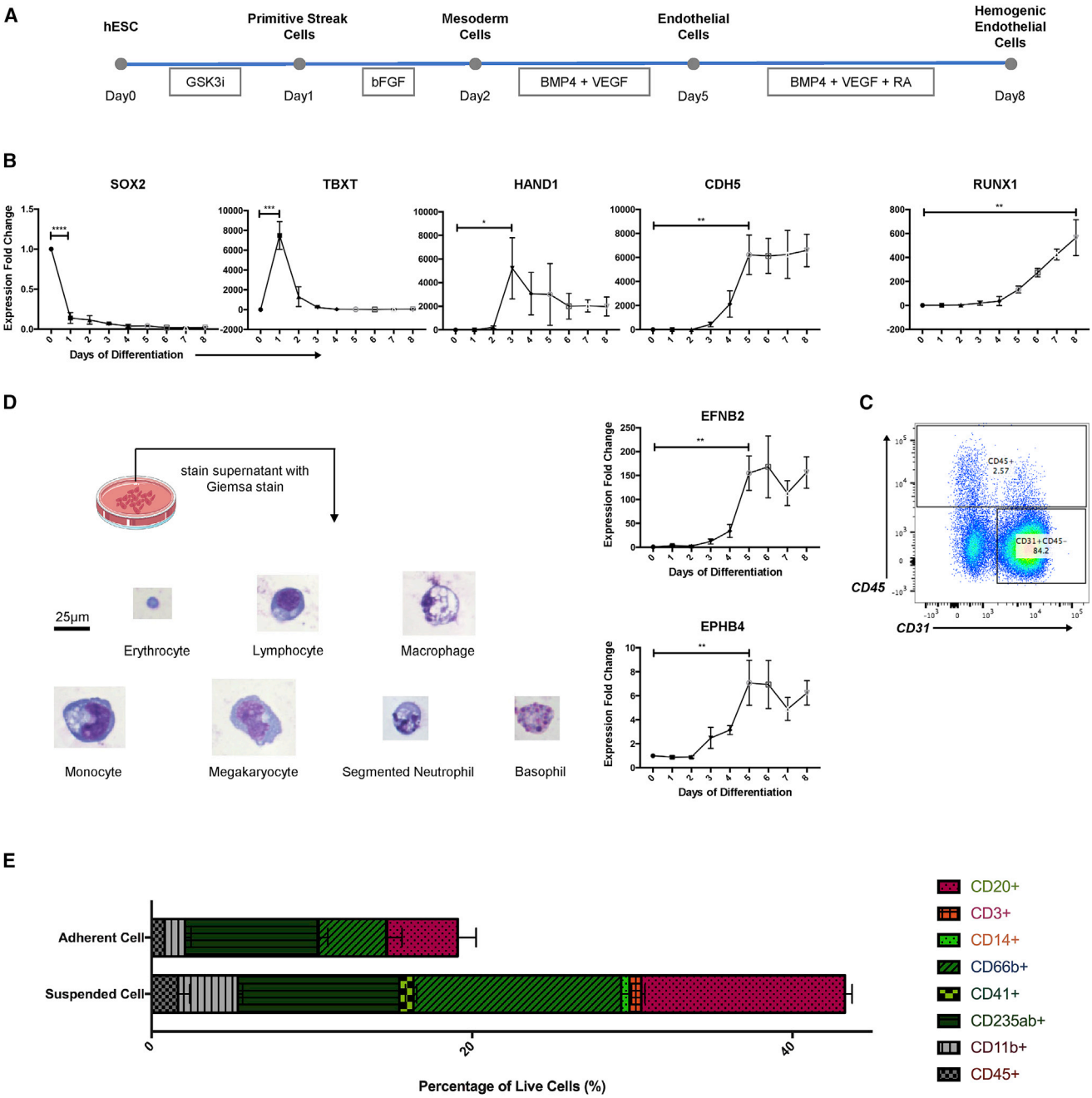

Figure 1. Simple *In Vitro* System to Derive Human Hemogenic Endothelial Cells from Human Embryonic Stem Cells (hESCs)

(A) Schematic representation of differentiation protocol, partially adapted from Sriram et al. (2015).

(B) qPCR analysis of markers associated with pluripotency (SOX2), primitive streak/early mesoderm (TBXT), mesoderm (HAND1), endothelium (CDH5), arterial endothelium (EFNB2), venous endothelium (EPHB4), and hematopoiesis (RUNX1); n = 3 for all groups. Student's t test: $p < 0.0001$ (SOX2), $p = 0.0008$ (TBXT), $p = 0.0253$ (HAND1), $p = 0.0028$ (CDH5), $p = 0.0018$ (EFNB2), $p = 0.0049$ (EPHB4), $p = 0.0029$ (RUNX1).

(C) Flow cytometry result showed generation of endothelial cells ($CD31^+CD45^-$) and blood cells ($CD45^+$) on day 8 (D8).

(D) Giemsa staining revealed generation of all blood cell lineages. Original magnification, 40×. Scale bar, 25 μm.

(E) Flow cytometry result showed generation of multi-lineage blood cells.

Data are represented as means ± SDs.

Among them, hematopoietic potential (colony-forming ability) was enriched within the KIT^+ and $CD34^+$ populations (Figures 2E and S3C). Lastly, we isolated $CD31^+CD45^-CDH5^-KIT^+CD34^+$ cells and found that hematopoietic potential was enriched within the kinase insert domain receptor-positive (KDR^+) population (Figures 2F and S3D–S3H). Thus, the $CD31^+KDR^+KIT^+CD34^+CDH5^-CD45^-$

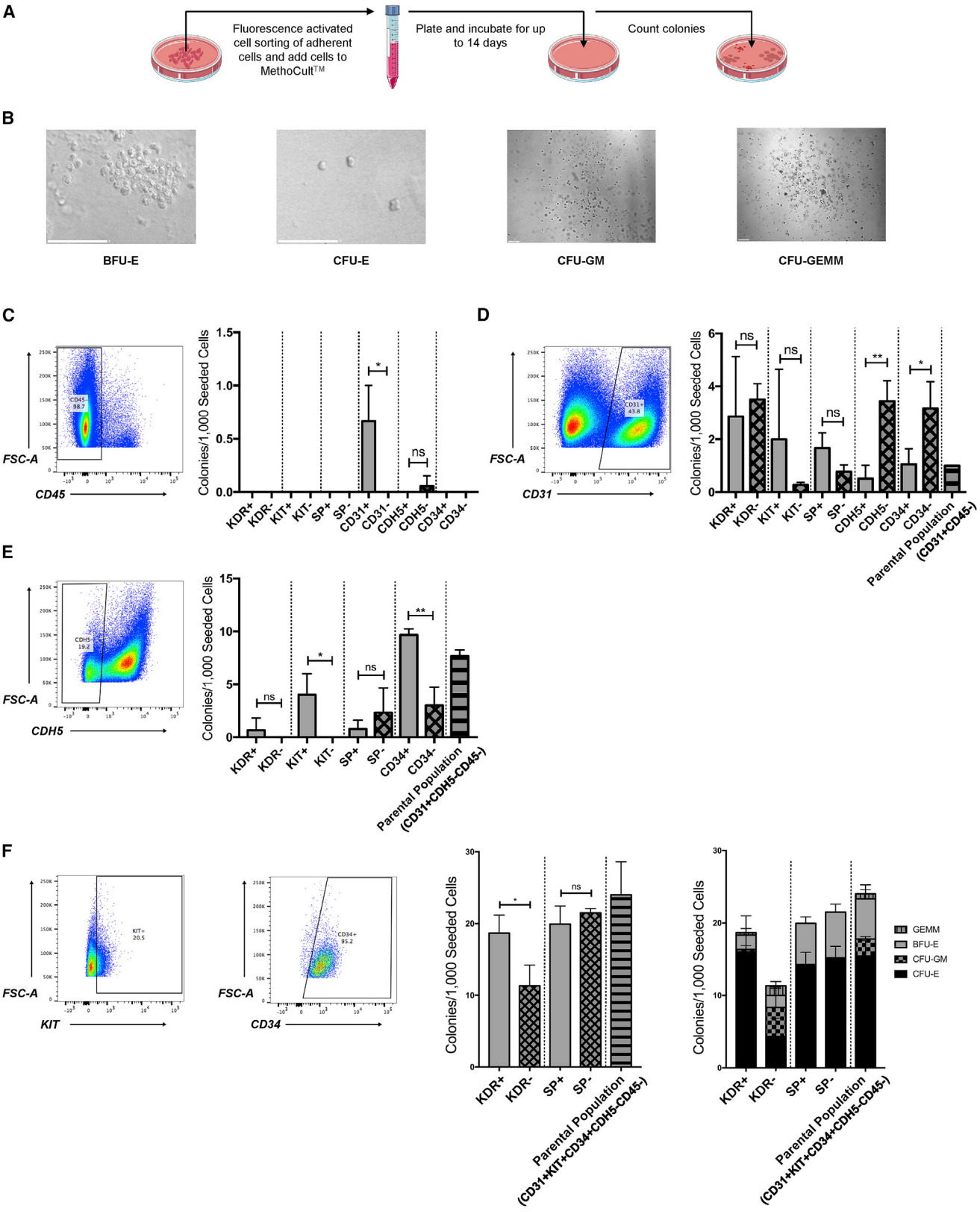

(legend on next page)

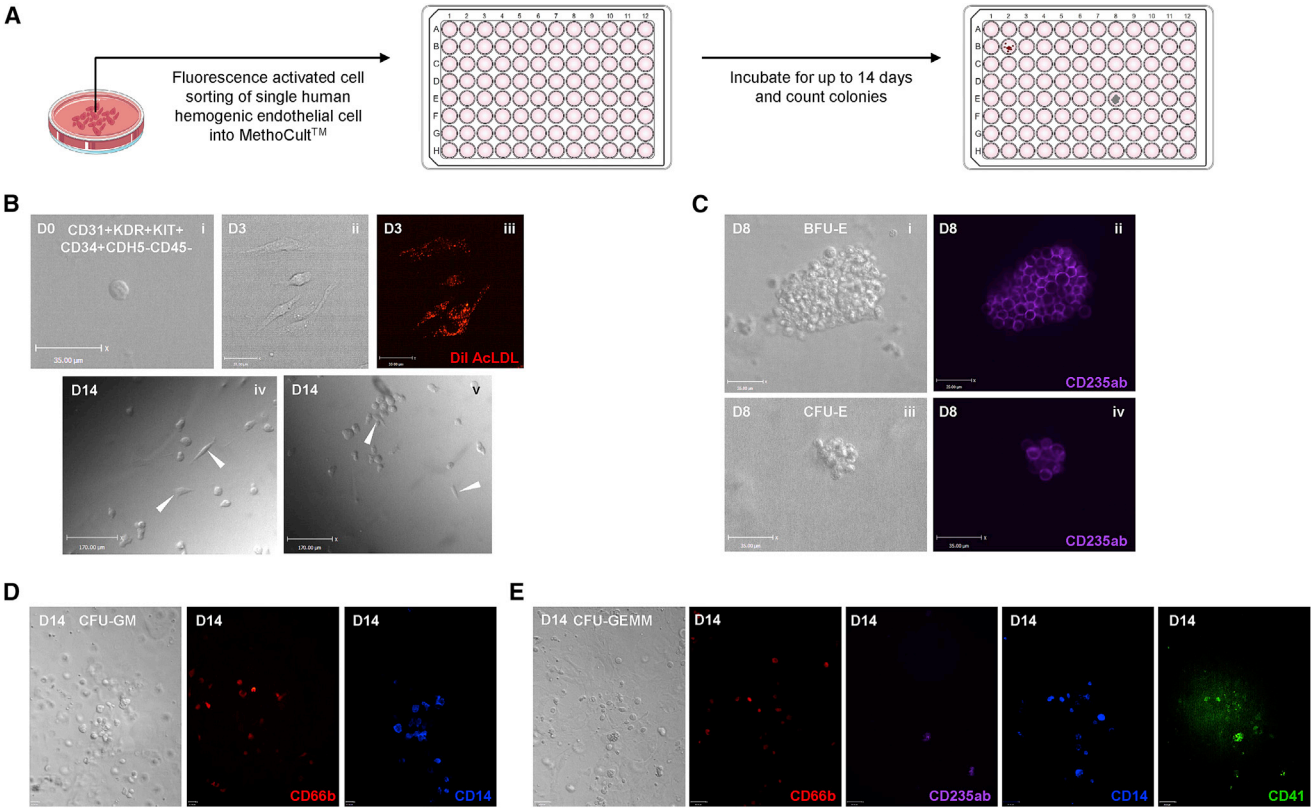

Figure 3. Characterization of the Phenotype of Human Hemogenic Endothelial Cells on a Single-Cell Level

(A) Schematic representation of single-cell blood-forming assay.

(B) Representative photographs showing single human hemogenic endothelial cell on D0 (i), hemogenic endothelial cell colony on D3 (ii), DiI AcLDL uptake of hemogenic endothelial cells on D3 (iii), and adherent hemogenic endothelial cells among blood cells on D14 (iv and v). Scale bars, 35 μm for (i), (ii), and (iii). Scale bars, 170 μm for (iv) and (v).

(C) Representative photographs showing BFU-E (i and ii) and CFU-E (iii and iv) on D8, marked by CD235ab. Scale bars, 35 μm.

(D) Representative photographs showing CFU-GM on D14, marked by CD66b and CD14. Scale bars, 35 μm.

(E) Representative photographs showing CFU-GEMM on D14, marked by CD66b, CD235ab, CD14, and CD41. Scale bars, 70 μm.

population of hESC-derived cells is highly enriched for human hemogenic endothelial cells (Figure S3H).

Upon characterizing these cells on a population level, we further evaluated their hematopoietic potential on a clonal level (Figure 3A). Single human hemogenic endothelial cells ($CD31^+KDR^+KIT^+CD34^+CDH5^-CD45^-$) were FACS sorted into 96-well plates on D0 (Figure 3Bi). By D3, small endothelial cell colonies formed. These cells not only demonstrated the typical cobblestone morphology (Figure 3Bii) but also the functionality of acetelyated, fluorescently labeled low-density lipoprotein (DiI AcLDL) uptake (Figure 3Biii) and the expression of endothelial nitric oxide synthase (eNOS) (Data S1, Data S2, and Data S3), which are characteristics of endothelial cells. Although some mature blood cells, such as monocytes or macrophages, can

Figure 2. Characterization of the Phenotype of Human Hemogenic Endothelial Cells on a Population Level

(A) Schematic representation of blood-forming assay.

(B) Representative photographs showing morphology of BFU-E erythroid colony, CFU-E erythroid colony, CFU-GM granulocyte-monocyte colony, and CFU-GEMM multipotent hematopoietic progenitor colony. Scale bars, 100 μm.

(C) Among non-HSPC ($CD45^-$), hematopoietic potential is enriched within the $CD31^+$ population; n = 3 for all groups. Student's t test: p = 0.03. Solid bars represent positive groups. Checkered bars represent negative groups. Striped bars represent parental groups.

(D) Among $CD31^+CD45^-$ cells, hematopoietic potential is enriched within the $CDH5^-$ and $CD34^-$ populations; n = 3 for all groups. Student's t test: p = 0.005 (CDH5), p = 0.04 (CD34). Solid bars represent positive groups. Checkered bars represent negative groups. Striped bars represent parental groups.

(E) Among $CD31^+CDH5^-CD45^-$ cells, hematopoietic potential is enriched within the KIT^+ and $CD34^+$ populations; n = 3 for all groups. Student's t test: p = 0.03 (KIT), p = 0.003 (CD34). Solid bars represent positive groups. Checkered bars represent negative groups. Striped bars represent parental groups.

(F) Among $CD31^+KIT^+CD34^+CDH5^-CD45^-$ cells, hematopoietic potential is enriched within the KDR+ population (~85% CFU-E, 2% BFU-E, 11% CFU-GM, 2% CFU-GEMM); n = 3 for all groups. Student's t test: p = 0.03. Unless labeled otherwise, solid bars represent positive groups. Checkered bars represent negative groups. Striped bars represent parental groups.

Data are represented as means ± SDs.

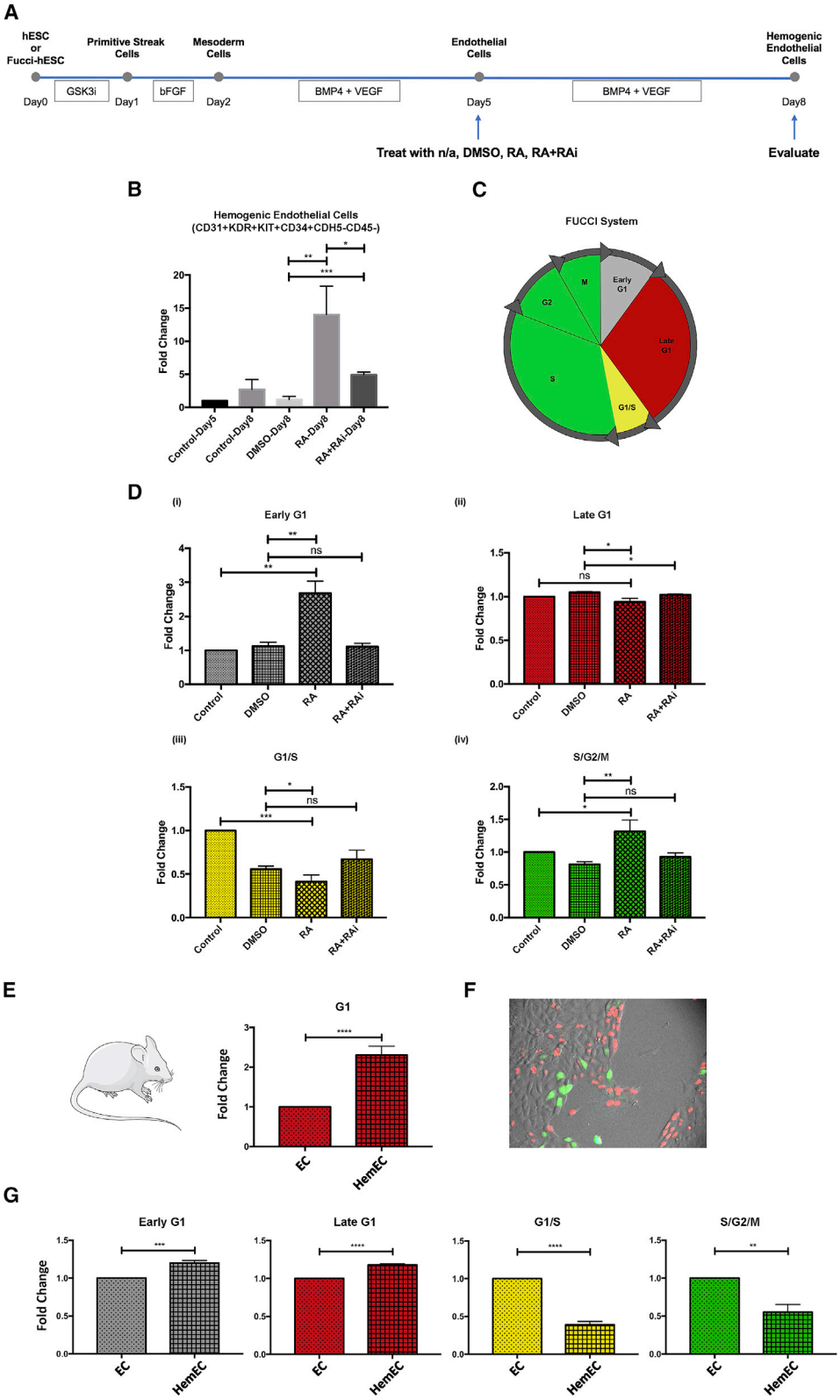

(legend on next page)

also take up DiI AcLDL, they were FACS excluded from the population tested in this assay, which contained only $CD45^-$ cells. Thus, these data show that human hemogenic endothelial cells derived from hESCs are able to proliferate in culture and maintain the characteristics of endogenous vascular endothelial cells. By D14, endothelial cells could still be observed among the hematopoietic colonies (Figure 3Biv and v). We further confirmed the identity of various hematopoietic colonies that single hESC-derived hemogenic endothelial cells were capable of giving rise to using immunostaining. These colonies include BFU-E erythroid colonies marked by CD235ab expression (Figure 3Ci and ii), CFU-E erythroid colonies marked by CD235ab expression (Figure 3Ciii and iv), CFU-GM colonies marked by CD66b and CD14 expression (Figure 3D), and CFU-GEMM multipotent hematopoietic progenitor colonies marked by the expression of CD66b, CD235ab, CD14, and CD41 (Figure 3E). Overall, we demonstrated that these hESC-derived $CD31^+KDR^+KIT^+CD34^+CDH5^-CD45^-$ human hemogenic endothelial cells exhibit multi-lineage hematopoietic potential on both population and single-cell levels.

RA Promotes Early G1 Cell Cycle State of hESC-Derived Endothelial Cells and the Enrichment of Hemogenic Endothelial Cells

To determine whether RA could enhance the specification of human hemogenic endothelial cells, we compared untreated hESC-derived endothelial cells (control group) to similar cells treated at D5 with vehicle (DMSO group) or RA (RA group), and quantified hemogenic endothelial cell generation on D8 of differentiation (Figure 4A). We used both control and DMSO groups because DMSO was previously shown to increase pluripotent stem cell differentiation (Chetty et al., 2013). We found that after 72 h of treatment, RA significantly increased the differentiation of hESC-derived human hemogenic endothelial cells, whereas DMSO had no effect (Figures 4B and S4A). When cells were treated with both RA and a RA receptor (RAR) pan-antagonist (RAi), RA-induced human hemogenic endothelial cell specification was largely blocked (Figures 4B and S4A).

We previously found that cell cycle state plays a critical role in murine arterial and hemogenic endothelial cell specification *in vivo* (Fang et al., 2017; Marcelo et al., 2013b). Here, we investigated the effect of RA on cell cycle distribution *in vitro* using H9-hESCs carrying the fluorescent ubiquitination-based cell cycle indicator (FUCCI) (H9-FUCCI-hESC reporter cell line) (Pauklin and Vallier, 2013). The FUCCI system uses antiphase oscillating proteins to mark distinct cell cycle states with fluorescent indicators, and cell cycle distribution can be analyzed via flow cytometry (Figure 4C) (Sakaue-Sawano et al., 2008). We found that RA treatment significantly increased the proportion of hESC-derived endothelial cells in early G1 phase and decreased the proportion transitioning from G1 to S phase (Figures 4D, S4B, and S4C). We also found that DMSO significantly increased the proportion of cells in late G1 phase (data not shown), which is consistent with previous findings (Chetty et al., 2013). When cells were treated with both RA and RAi, RA-induced changes in the cell cycle state were suppressed. These data show that RA promotes the differentiation and enrichment of hemogenic endothelial cells from hESCs, and this is accompanied by an increased proportion of cells in early G1 phase and a decreased proportion transitioning from G1 to S phase.

Mouse and Human Hemogenic Endothelial Cells Are Predominantly in G1 Cell Cycle State *In Vivo* and *In Vitro*

Our previous studies of murine yolk sac and AGM endothelial cells (Marcelo et al., 2013b), and the studies above in hESC-derived endothelial cells, demonstrate that in both model systems, RA promotes hemogenic specification, as well as cell cycle arrest. To further define the cell cycle state of murine hemogenic endothelial cells versus non-blood-forming endothelial cells *in vivo* during definitive hematopoiesis, we used FUCCI-red mice, carrying mKO fluorescent protein that marks cells in G1 phase (Sakaue-Sawano et al., 2008). Using flow cytometry, we isolated murine E10.5 AGM endothelial cells ($CD31^+CD45^-SP^-$) and hemogenic endothelial cells ($Flk\text{-}1^+Kit^+CD45^-SP$) and found that the proportion of hemogenic endothelial cells in G1 phase was significantly higher than in non-blood-forming endothelial cells in the AGM (Figures 4E and S5A). To further define the cell cycle state of hESC-derived human hemogenic endothelial cells, we used the H9-FUCCI-hESCs described above (shown in Figure 4F) (Pauklin and Vallier, 2013), which can clearly delineate cells in early G1, late G1, G1-to-S, and S/G/M phases (depicted in Figure 4C). We found that compared to total human endothelial cells ($CD31^+CD45^-$), a

Figure 4. RA Promotes Early G1 Cell Cycle State of hESC-Derived Endothelial Cells and Their Specification toward Hemogenic Endothelial Cells

(A) Schematic representation of experimental design.

(B) RA induces differentiation of hemogenic endothelial cells; n = 3 for all groups. Student's t test: p = 0.0068 (DMSO versus RA), p = 0.0005 (DMSO versus RA^+RAi), p = 0.0218 (RA versus RA^+RAi).

(C) Schematic representation of the cell cycle states observable using the FUCCI system.

(D) RA induces early G1 cell cycle enrichment in endothelial cells. Cell cycle distribution was measured by expression of the FUCCI reporter construct using flow cytometry; n = 3 for all groups. (i) Student's t test: p = 0.0012 (control versus RA), p = 0.0019 (DMSO versus RA). (ii) Student's t test: p = 0.0122 (DMSO versus RA), p = 0.0102 (DMSO versus RA+RAi). (iii) Student's t test: p = 0.0002 (control versus RA), p = 0.0389 (DMSO versus RA). (iv) Student's t test: p = 0.0355 (control versus RA), p = 0.0084 (DMSO versus RA).

(E) In E10.5 mouse AGM, significantly more hemogenic endothelial cells were in late G1 phase compared to non-blood-forming endothelial cells; n = 4 for all groups. Student's t test: $p < 0.0001$.

(F) Picture of H9-FUCCI-hESC-derived endothelial cells. Original magnification, 20×.

(G) In hESC culture on D8, significantly more hemogenic endothelial cells were in early and late G1 compared to non-blood-forming endothelial cells; n = 3 for all groups. Student's t test: p = 0.0005 (early G1), $p < 0.0001$ (late G1), $p < 0.0001$ (G1/S), p = 0.0016 (S/G2/M).

Data are represented as means ± SDs.

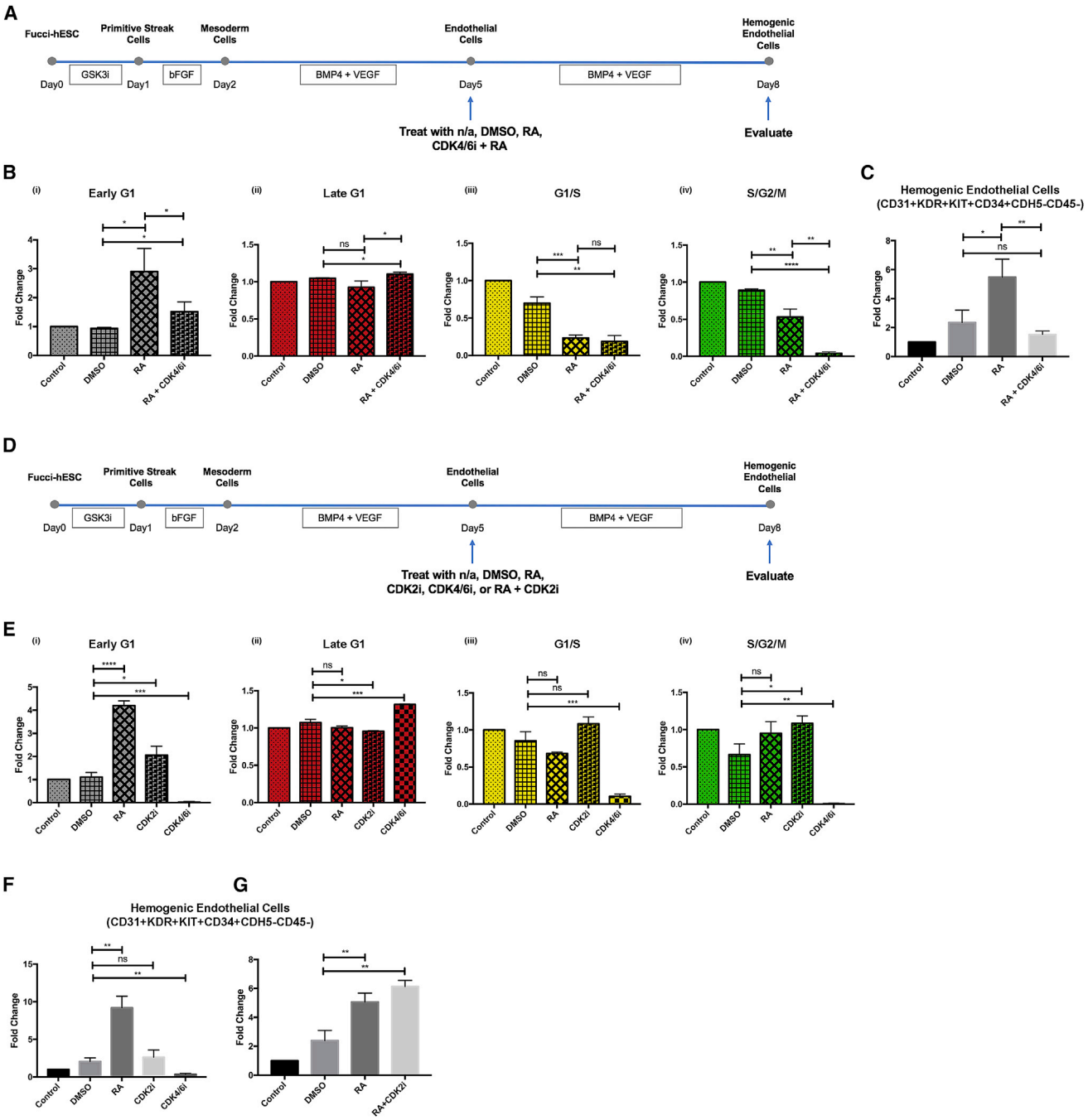

Figure 5. Early G1 Cell Cycle State of Endothelial Cells Is Necessary but Not Sufficient to Enable Hemogenic Specification

(A) Schematic representation of experimental design.

(B) When cells were treated with both RA and CDK4/6i, CDK4/6i overrides effect of RA on cell cycle state and enriches endothelial cells in late G1 phase. Cell cycle distribution was measured by expression of the FUCCI reporter construct using flow cytometry; n = 3 for all groups. (i) Student's t test: p = 0.0130 (DMSO versus RA), p = 0.0423 (DMSO versus RA$^+$CDK4/6i), p = 0.0497 (RA versus RA$^+$CDK4/6i). (ii) Student's t test: p = 0.0205 (DMSO versus RA$^+$CDK4/6i), p = 0.0253 (RA versus RA$^+$CDK4/6i). (iii) Student's t test: p = 0.0010 (DMSO versus RA), p = 0.0016 (DMSO versus RA$^+$CDK4/6i). (iv) Student's t test: p = 0.0046 (DMSO versus RA), p < 0.0001 (DMSO versus RA$^+$CDK4/6i), p = 0.0015 (RA versus RA$^+$CDK4/6i).

(C) In the absence of early G1 cell cycle arrest in endothelial cells, RA$^+$CDK4/6i could not induce hemogenic endothelial cell specification; n = 3 for all groups. Student's t test: p = 0.0233 (DMSO versus RA), p = 0.0059 (RA versus RA$^+$CDK4/6i).

(D) Schematic representation of experimental design.

(E) Similar to RA, CDK2i induces early G1 cell cycle arrest in endothelial cells. Cell cycle distribution was measured by expression of the FUCCI reporter construct using flow cytometry; n = 3 for all groups. (i) Student's t test: p < 0.0001 (DMSO versus RA), p = 0.0196 (DMSO versus CDK2i), p = 0.0007 (DMSO versus CDK4/6i).

(legend continued on next page)

significantly greater proportion of human hemogenic endothelial cells ($CD31^+KDR^+KIT^+CD34^+CDH5^-CD45^-$) were also in G1 phase and a significantly lower proportion were actively cycling (Figures 4G and S5B). Overall, these studies implicate a role for cell cycle state in human hemogenic endothelial cell specification and highlight a potentially conserved developmental paradigm in mice and humans.

Early G1 Cell Cycle State Is Necessary but Not Sufficient to Enable Hemogenic Endothelial Cell Specification

We found that hemogenic endothelial cells *in vivo* and *in vitro* were predominantly in G1 phase, and G1 arrest is required for murine hemogenic endothelial cell specification (Marcelo et al., 2013b). In addition, RA treatment, which promoted human hemogenic endothelial cell development, specifically increased the proportion of hESC-derived endothelial cells in early G1 phase, and concomitantly decreased the proportion of cells exiting G1 phase. Therefore, we specifically focused on the role of G1 state in hemogenic specification, and tested whether early G1 versus late G1 cell cycle state is necessary for hemogenic specification. To do so, we treated endothelial cells with a CDK4/6 inhibitor (CDK4/6i), which causes an accumulation of cells specifically in late G1 phase (Schmidt and Sebastian, 2018), and tested their response to RA (Figure 5A). As expected, RARACDK4/6i treatment increased the proportion of endothelial cells in late G1 phase (Figures 5Bii and S6Aii). In contrast, RA treatment alone increased the proportion of endothelial cells in early G1 phase (Figures 5Bi and S6Ai), consistent with the studies described above. The effects of RA and CDK4/6i on G1/S and S/G2/M phases were comparable (Figures 5Biii, 5Biv, S6Aiii, and S6Aiv). When hESC-derived endothelial cells were arrested in late G1 phase, as opposed to early G1 phase, hemogenic endothelial cell specification was suppressed even in the presence of RA (Figures 5C and S6B). Thus, the early G1 cell cycle state appears to be necessary for RA-induced hemogenic endothelial cell specification. Of note, we did not test the potential role of S/G2/M states for several reasons: a low proportion (<10%, data not shown) of hemogenic endothelial cells reside in this state *in vivo* and *in vitro*, we cannot verify arrest in S versus G2 versus M using this FUCCI reporter cell line, and the drugs available to arrest cells in these phases are associated with confounding effects such as cytotoxicity, increased apoptosis, and chromosome damage.

To test whether the early G1 cell cycle state in endothelial cells is sufficient for hemogenic specification, hESC-derived endothelial cells were treated with either RA, CDK4/6i, or CDK2 inhibitor (CDK2i), which arrests cells specifically in early G1 phase of the cell cycle (Chao et al., 2019) (Figure 5D). The CDK2i (CVT-313) that we used is a cell-permeable purine analog that acts as a potent and selective ATP-competitive inhibitor of CDK2, which inhibits other kinases only at much higher concentrations. As expected, and similar to RA, CDK2i increased the proportion of endothelial cells in early G1 phase (Figures 5Ei and S7Ai); in contrast, CDK4/6i increased the proportion of endothelial cells in late G1 phase (Figures 5Eii and S7Aii). We found that arresting endothelial cells in either early G1 or late G1 alone (in the absence of RA treatment) was not sufficient to promote hemogenic specification (Figures 5F and S7B). In addition, when hESC-derived endothelial cells were treated with both RA and CDK2i, there was a trend toward an increase in hemogenic endothelial cell specification (Figures 5G and S7C). Thus, early G1 cell cycle arrest of human endothelial cells is necessary but not sufficient to promote hemogenic specification.

Bulk RNA Sequencing (RNA-Seq) Reveals Candidates of Additional Signals That RA Provides to Promote Hemogenic Endothelial Cell Specification

To gain further mechanistic insight into the role of RA during human hemogenic endothelial cell specification, we performed bulk RNA-seq of H1-hESC-derived endothelial cells ($CD31^+CD45^-$) treated with or without RA (Figure 6A). Both control (Figure 6Bi) and RA-treated (Figure 6Bii) endothelial cells ($CD31^+CD45^-$) were FACS isolated on D8 and subjected to bulk RNA-seq.

We identified 2,547 genes significantly downregulated and 2,208 genes significantly upregulated in RA-treated endothelial cells, and performed gene set enrichment analysis of the datasets, respectively. We found that genes downregulated by RA were strongly associated with the vascular endothelial growth factor (VEGF) signaling pathway, which plays an essential role in endothelial cell proliferation and arterial specification (Bernatchez et al., 1999; Lawson et al., 2002) (Figure 6C). Transcription factors associated with these genes include ETV2, which is necessary for endothelial cell differentiation (De Val and Black, 2009), and KLF5, which promotes endothelial cell proliferation via the regulation of VEGF (Gao et al., 2015; Nagai et al., 2005). In addition, our analysis revealed a shift away from an endothelial phenotype upon RA treatment, demonstrated by the downregulation of genes associated with KDR expression and a human umbilical vein endothelial cell (HUVEC) phenotype. Lastly, the gene set enrichment analysis results further confirmed the role of RA in cell cycle regulation. Genes downregulated by RA are linked to transcription factor E2F1, which promotes the G1-to-S phase transition (Poppy Roworth et al., 2015).

In contrast, we found that genes upregulated by RA treatment were strongly associated with RA signaling (as expected), as well as Notch, Wnt and Hedgehog (HH) signaling. Notch is known to promote murine hemogenic specification downstream of RA (Marcelo et al., 2013b), and these results suggest conserved

(ii) Student's t test: p = 0.0115 (DMSO versus CDK2i), p = 0.0007 (DMSO versus CDK4/6i). (iii) Student's t test: p = 0.0005 (DMSO versus CDK4/6i). (iv) Student's t test: p = 0.0148 (DMSO versus CDK2i), p = 0.0014 (DMSO versus CDK4/6i).

(F) Unlike RA, CDK2i could not induce hemogenic endothelial cell specification; n = 3 for all groups. Student's t test: p = 0.0016 (DMSO versus RA), p = 0.0051 (DMSO versus CDK4/6i).

(G) CDK2i did not artificially suppress cell growth or cell differentiation in culture. Student's t test: p = 0.0077 (DMSO versus RA), p = 0.0015 (DMSO versus RA^+CDK2i).

Data are represented as means ± SDs.

A

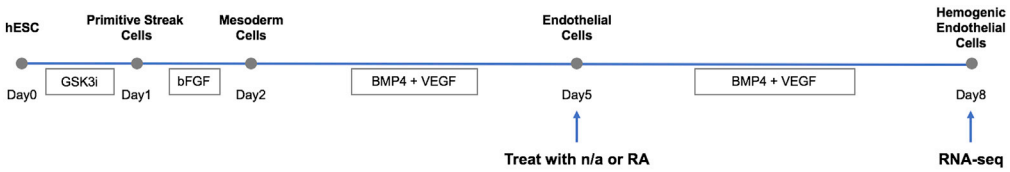

B

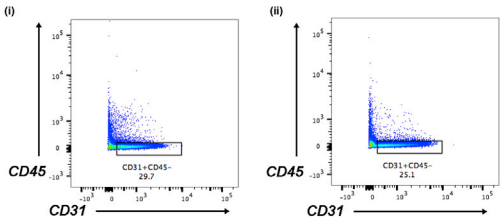

C

Gene Set Enrichment Analysis – RA Downregulated

Category	Database	
Transcription	TF Perturbations Followed by Expression	ETV2 OE HESC HUMAN GSE57395 RNASEQ UP 1.131e-83
	TRRUST Transcription Factors 2019	E2F1 human 3.844e-7
	TRANSFAC and JASPAR PWMs	KLF5 (human) 1.887e-7
		E2F1 (human) 4.768e-7
Pathways	WikiPathways 2019 Human	VEGFA-VEGFR2 Signaling Pathway WP3888 2.077e-21
	ARCHS4 Kinases Coexp	KDR human kinase ARCHS4 coexpression 1.356e-54
	Reactome 2016	Signaling by VEGF Homo sapiens R-HSA-194138 2.506e-29
		VEGFA-VEGFR2 Pathway Homo sapiens R-HSA-4420097 1.311e-28
	NCI-Nature 2016	Signaling events mediated by VEGFR1 and VEGFR2 Homo sapiens d6f6ae1f-6195-11e5-8ac5-06603eb7f303 4.532e-12
Cell types	ARCHS4 Cell-lines	HUVEC 2.628e-142

D

Gene Set Enrichment Analysis – RA Upregulated

Category	Database	
Transcription	ENCODE and ChEA Consensus TFs from ChIP-X	SOX2 CHEA 2.087e-9
		TRIM28 CHEA 0.00002054
		SMAD4 CHEA 0.00004124
	Transcription Factor PPIs	SMAD1 2.740e-7
		SMAD3 2.222e-7
		SMAD4 0.00002642
		SMAD2 0.00001645
Pathways	BioPlanet 2019	Maturation of Notch precursor via proteolytic cleavage 0.0006756
		Retinoic acid receptor-mediated signaling 0.0002142
		Signaling events mediated by the hedgehog family 0.0004611
	WikiPathways 2019 Human	Hedgehog Signaling Pathway WP4249 0.000009306
		Hedgehog Signaling Pathway WP47 0.00001327
	KEGG 2019 Human	Hedgehog signaling pathway 0.000005345
	Elsevier Pathway Collection	Hedgehog Family -> ARRB1/ARRB2 Canonical Signaling 0.00001327
		Hedgehog Family Signaling 0.000006945
		NOTCH Receptors Signaling 0.00002718
	NCI-Nature 2016	Signaling events mediated by the Hedgehog family Homo sapiens d3a49cee-6195-11e5-8ac5-06603eb7f303 0.0003110
		Retinoic acid receptors-mediated signaling Homo sapiens 5797691b-6195-11e5-8ac5-06603eb7f303 0.0005292
		Wnt signaling network Homo sapiens 987a2b9f-6196-11e5-8ac5-06603eb7f303 0.002339
	Panther 2016	Hedgehog signaling pathway Homo sapiens P00025 0.002091
		Notch signaling pathway Homo sapiens P00045 0.002054
		Wnt signaling pathway Homo sapiens P00057 0.0003476
	PPI Hub Proteins	SMAD3 0.00001575
		SMAD1 0.0001645
Cell Types	Human Gene Atlas	CD8+ T cells 2.130e-7
		CD4+ T cells 0.000008630

E

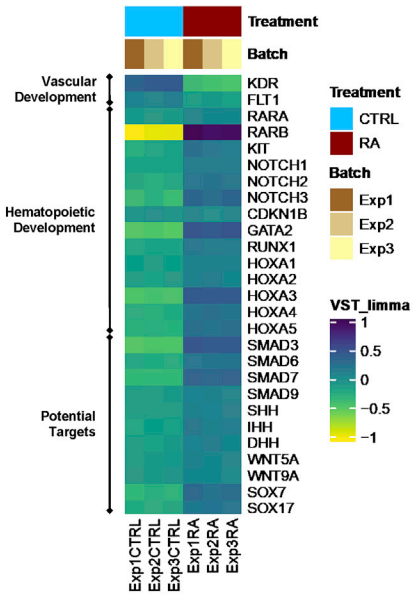

(legend on next page)

molecular regulation of mouse and human hemogenic endothelial cell specification. Wnt signaling has long been recognized as an important regulator of hematopoiesis. More specifically, canonical Wnt signaling plays an important role in maintaining hematopoietic stem cell (HSC) self-renewal, and has also been shown to interact with other signaling pathways, including HH and Notch (Staal and Luis, 2010) (Figure 6D). SMAD factors are also significantly upregulated with RA treatment. They play a critical role in regulating endothelial cell growth suppression (Bohnsack et al., 2004), as well as the fate of HSPCs during development and postnatally, by mediating transforming growth factor β (TGF-β) signaling (Larsson and Karlsson, 2005). Lastly, genes upregulated by RA are also associated with SOX2 and TRIM28 activities, and both have been shown to support the early stages of blood cell development (Hosoya et al., 2013; Sarkar and Hochedlinger, 2013).

We further examined RA regulation of genes known to be involved in vascular development and hemogenic specification (Figure 6E). Similar to our findings above, RA treatment led to a shift away from endothelial phenotype and toward a hematopoietic phenotype. More specifically, RA suppressed the expression of VEGF receptors KDR and Fms-related receptor tyrosine kinase 1 (FLT1), which are important for endothelial cell proliferation and maintenance (Melincovici et al., 2018). In contrast, RA upregulated the expression of a number of genes associated with murine hemogenic endothelial cells and HSPCs, including RAR, KIT, NOTCH, CDKN1B, GATA2 and RUNX1. In addition, the expression of a number of SMAD family members was upregulated, as were ligands of the HH and Wnt signaling pathways, and homeobox A1 (HOXA1) genes that are known to play a role in hematopoietic development (Alsayegh et al., 2019). These results are consistent with the gene set enrichment analyses, and suggest that there is potential crosstalk among the RA/HOX/SMAD/HH/Wnt signaling pathways that instructs the hemogenic specification of endothelial cells and concomitant downregulation of endothelial cell identity.

RNA-Seq Analysis Provides Insights That Link Endothelial Cell Cycle State to Hemogenic Specification

To gain further mechanistic insight into the role of cell cycle regulation in human hemogenic endothelial cell specification, we performed bulk RNA-seq of H9-FUCCI-hESC-derived endothelial cells ($CD31^+CD45^-$) in distinct cell cycle states (Figure 7A). Cells in early G1, late G1, G1/S, and S/G2/M phases were FACS isolated and subjected to bulk RNA-seq (Figure 7B). We identified genes exclusively upregulated in early G1 phase (1,854 genes) and late G1 phase (2,387 genes) and performed gene set enrichment analysis. Genes exclusively upregulated in early G1 were predominantly associated with hematopoietic development, and hESC-derived endothelial cells in early G1 phase showed high resemblance to cell types such as MOLT-4 cell (T lymphoblast), erythroid cell, B lymphoblast, and cord blood (Figure 7C). In contrast, genes exclusively upregulated in late G1 were predominantly linked to vascular development and angiogenesis, while some genes were associated with heart, ventricle, atrium, placenta, whole blood, and monocytes (Figure 7C).

To further investigate the link between endothelial cell cycle state and cell fate decisions, we examined the differential expression of specific genes associated with vascular development, hemogenic specification, and arterial specification in endothelial cells in distinct cell-cycle states (Figure 7D). We found an enrichment of genes associated with hemogenic specification in early G1 phase (e.g., CDKN1B, ESAM, HES1, GATA2, TAL1, LMO2) (Figure 7E). In contrast, we observed an enrichment of genes associated with arterial specification in late G1 phase (e.g., GJA4, GJA5, NRP1, EFNB2, DLL4, TGFBR2) (Figure 7F), which is consistent with our previous findings in murine arterial endothelial cell specification (Fang et al., 2017).

Our studies suggest that RA plays a dual role in human hemogenic endothelial cell specification. That is, it promotes endothelial cell arrest in early G1 phase, which is necessary to enable hemogenic specification (Figure 7G), and also induces signaling pathways that are necessary for altering gene expression, specifically in early G1 state, to promote a hemogenic phenotype and suppress endothelial cell identity.

DISCUSSION

Previous studies have demonstrated the endothelial origin of blood cells *in vivo* (Marcelo et al., 2013a; Medvinsky and Dzierzak, 1996; Taoudi and Medvinsky, 2007). Further mechanistic studies have shed light on how a subset of murine endothelial cells acquires hematopoietic potential, highlighting the critical role of the RA/Kit/Notch/p27 signaling pathway and cell cycle regulation (Goldie et al., 2008; Marcelo et al., 2013b). However, whether a specific cell cycle state is necessary for hemogenic specification of endothelial cells or whether this mechanism is conserved in humans was unknown. In these studies, we established a simple *in vitro* system to derive human endothelial and hemogenic endothelial cells and delineate their mechanism(s) of development.

Compared to existing systems that can be used to derive endothelial and hematopoietic cells from hESCs, our system has several advancements. For example, it does not require

Figure 6. Bulk RNA Sequencing Reveals Candidate Mediators of RA Regulation of Human Endothelial Cell Cycle Control and Hemogenic Specification

(A) Schematic representation of experimental design.

(B) Endothelial cells ($CD31^+CD45^-$) treated with (i) n/a or (ii) RA were collected on D8 for RNA sequencing using FACS sorting.

(C) Gene set enrichment analysis was performed for genes exclusively downregulated in RA-treated endothelial cells. Relevant and significant ($p < 0.05$) terms are shown.

(D) Gene set enrichment analysis was performed for genes exclusively upregulated in RA-treated endothelial cells. Relevant and significant ($p < 0.05$) terms are shown.

(E) Selected markers demonstrate upregulation of genes associated with hematopoietic cell fate in endothelial cells by RA.

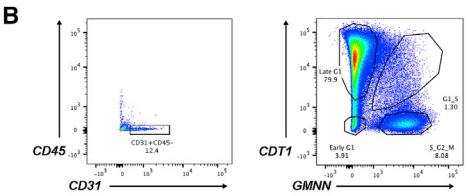

C

Gene Set Enrichment Analysis

Category	Early G1	Late G1
Ontology (Jensen TISSUES)	MOLT-4 cell 1.769e-61	Heart 1.871e-56
	Erythoid cell 4.297e-61	Cardiac muscle 1.250e-47
Ontology (GO Biological Process 2018)	Regulation of hematopoietic stem cell differentiation 8.477e-11	Regulation of angiogenesis 3.298e-8
	Regulation of stem cell differentiation 1.602e-10	Cellular response to TGF-beta stimulus 1.181e-7
Pathway (Panther 2016)	Ubiquitin proteasome pathway 0.001487	Angiogenesis 0.000001054
	Transcription regulation by bZIP transcription factor 0.03678	VEGF signaling pathway 0.000007777
		Notch signaling pathway 0.00006770
Pathway (Kinase Perturbations from GEO up)	KIT active mutant 7.450e-12	BRAF drug inhibition 2.223e-19
Cell Type (Human Gene Atlas)	B lymphoblasts 2.584e-9	Placenta 1.439e-12
	CD34+ 0.00008890	Whole blood 4.573e-9
	CD71+ early erythroid 0.01977	CD14+ monocytes 8.456e-9
Cell Type (ARCHS4 Tissues)	CD34+ cells 3.055e-7	Ventricle 4.033e-25
	Cord blood 0.01513	Atrium 7.185e-15
		Heart 0.000007649

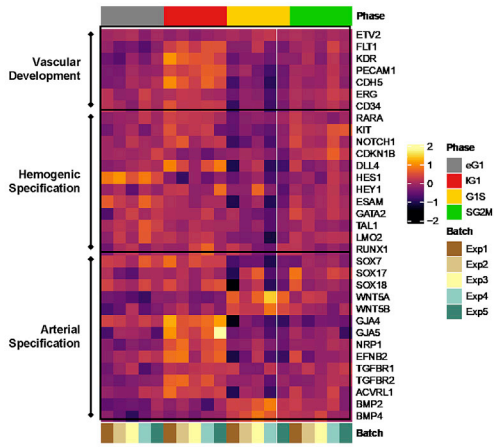

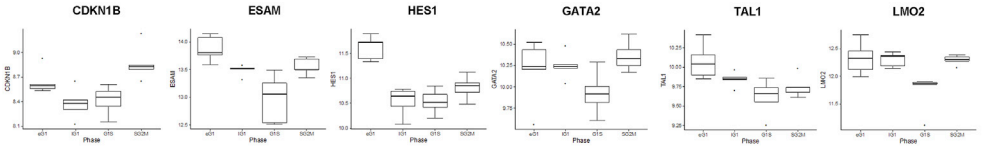

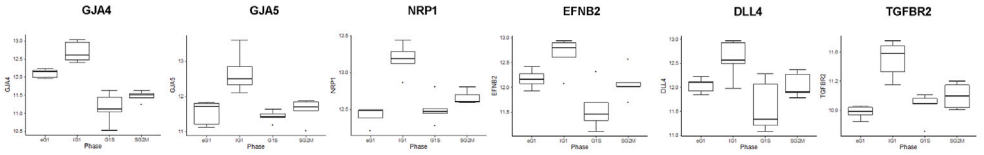

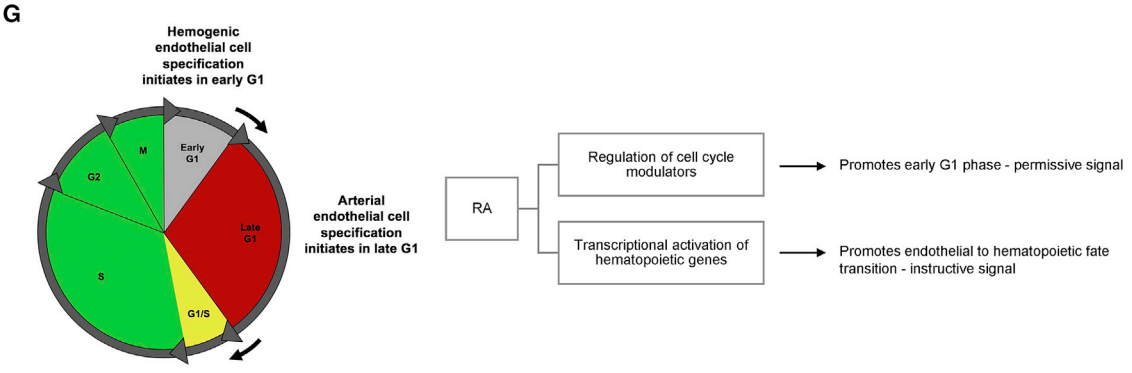

(legend on next page)

the use of mouse feeder cells or the formation of embryoid bodies, and is therefore less technically challenging to adopt. In addition, our system reduces the presence of other cell types and/or the development or other organ systems to provide a more controlled environment and consistency for molecular mechanistic studies. Our system also requires fewer growth factors and less time and is therefore more economical. Using this system, we showed that RA plays a critical role in the specification of human hemogenic endothelial cells, which we defined on a clonal level.

We propose that RA has two roles during hemogenic specification—promoting cell cycle arrest of endothelial cells in early G1 phase (permissive signal) and activating transcriptional programs (instructive signal) that enable the transition from endothelial to hemogenic endothelial cells, specifically in early G1. Thus, we hypothesize that arrest in early G1 state provides a distinct "window of opportunity" for endothelial cells to respond to external stimuli that promotes their specification toward a hemogenic endothelial cell phenotype. In addition, RA extends the window of time for hemogenic specification by enriching endothelial cells in early G1; RA also activates signaling pathways and transcriptional regulators that promote hemogenic specification in early G1. Consistent with this idea, others have shown that the cell cycle state determines the propensity for hESCs to commit to mesodermal versus endodermal and ectodermal lineages (Pauklin and Vallier, 2013).

We demonstrated that both of these functions of RA are required for hemogenic specification. To test the cell-cycle-regulation role of RA, we showed that chemically enriching endothelial cells in a different cell cycle phase (late G1 versus early G1 that is induced by RA) prevented hemogenic specification despite the presence of RA. To test the transcriptional role of RA, we demonstrated that chemically enriching endothelial cells in early G1 phase with CDK2i was not capable of inducing hemogenic specification in the absence of RA. These data show that both the cell cycle regulation and the transcriptional role of RA are necessary for hemogenic specification. Although hemogenic specification occurs while endothelial cell cycle progression is arrested, after specification, hemogenic endothelial cells must progress into S/G2/M states to divide and give rise to HSPCs. Thus, further understanding of cell cycle control throughout this endothelial-to-hematopoietic transition process is needed.

Our RNA-seq analyses revealed signaling pathway(s) and transcriptional regulators that RA may activate to enable cell cycle arrest and an endothelial to hemogenic endothelial cell fate transition. Interestingly, some of the same RA-induced pathways that regulate murine hemogenic specification, such as Notch and KIT, appear to be conserved in this process in human endothelial cells. Our analyses also revealed crosstalk with other pathways, including SMAD, Wnt, and HH signaling. Thus, it will be important in future studies to elucidate the exact roles of and potential interactions among these factors that may function downstream of RA to regulate the human endothelial cell cycle state and hemogenic specification.

It is not clear why hemogenic specification occurs in early G1 state of the endothelial cell cycle. Our RNA-seq data revealed enrichment of genes associated with hemogenic specification in early G1 phase and genes associated with arterial specification in late G1 phase, consistent with our previous studies (Fang et al., 2017). However, we also observed an enrichment of genes associated with hemogenic endothelial cells (e.g., NOTCH1, DLL4, HEY1, KIT, RUNX1) in late G1 phase. Thus, we propose that hemogenic specification initiates in early G1 and continues into late G1. Similarly, our data also suggest that arterial specification initiates in late G1 and continues into G1/S; that is, an enrichment of genes associated with arterial specification (e.g., BMP2, BMP4, BMP7, WNT2, WNT5B, WNT8A) was observed in G1/S phase in addition to late G1 phase. Other studies showed that expression of developmental regulators such as HOXD1, TBX5, and SOX11 is specifically upregulated in both early and late G1 phases (Singh et al., 2013). In contrast, human stem cells in S and G2 phases have been shown to possess an intrinsic tendency toward the pluripotent state (Gonzales et al., 2015). Despite recent discoveries linking cell cycle state to cell fate decisions in stem cells, understanding the molecular role of the cell cycle state during endothelial cell differentiation and hemogenic specification requires further investigation.

Finally, although our study focused on the process of hemogenic endothelial cell specification, cell cycle control has also been previously implicated in murine arterial endothelial cell specification (Fang et al., 2017), and our RNA-seq data suggest that this is conserved in human endothelial cell development. The use of emerging technologies such as single-cell RNA-seq will enable us to further delineate the heterogeneity within and phenotypic continuum among endothelial cell subtypes and their molecular regulators during their development. Such insights will improve our ability to apply developmental advances to the generation of distinct endothelial cell subtypes for tissue engineering and regenerative medicine. In addition, our system could likely be developed further to optimize the generation of transplantable HSPCs from human hemogenic endothelial cells for clinical therapies.

Figure 7. Bulk RNA Sequencing Provides Insights That Link Endothelial Cell Cycle State to Hemogenic Specification

(A) Schematic representation of experimental design.

(B) Endothelial cells ($CD31^+CD45^-$) in different cell cycle phases (early G1, late G1, G1/S, S/G2/M) were collected on D8 for RNA sequencing using FACS sorting.

(C) Gene set enrichment analysis was performed for genes exclusively upregulated in early and late G1 cell cycle phases. Relevant and significant ($p < 0.05$) terms are shown.

(D) Gene marker expression in various cell cycle phases.

(E) Selected markers demonstrate enrichment of genes associated with hematopoiesis in early G1 phase.

(F) Selected markers demonstrate enrichment of genes associated with vascular development and arterial endothelium in late G1 phase.

(G) Schematic representation of working model.

Data are represented as the highest/lowest value within 1.5x interquartile range (IQR) above/below the 75th/25th percentile.

STAR★METHODS

Detailed methods are provided in the online version of this paper and include the following:

- KEY RESOURCES TABLE
- RESOURCE AVAILABILITY
  - Lead Contact
  - Materials Availability
  - Data and Code Availability
- EXPERIMENTAL MODEL AND SUBJECT DETAILS
  - Cell culture
  - Animals
- METHOD DETAILS
  - Differentiation protocol
  - qPCR
  - Giemsa stain
  - Flow cytometry analysis for cell culture
  - Methylcellulose-based blood forming assay
  - Dil AcLDL uptake
  - Immunostaining of hematopoietic colonies
  - Flow cytometry analysis for animal tissue
- QUANTIFICATION AND STATISTICAL ANALYSIS
  - RNA sequencing
  - Statistical analysis

SUPPLEMENTAL INFORMATION

Supplemental Information can be found online at https://doi.org/10.1016/j.celrep.2020.108465.

ACKNOWLEDGMENTS

The authors would like to thank Dr. L. Vallier for providing H9-FUCCI-hESC. This work was funded by NIH grants HL128064 and U2EB017103 and the CT Innovations 15-RMB-YALE-04 grant to K.K.H.; NIH grants R01-AI130471 and R01-CA228019 and Merit Review award I01BX002919 from the Department of Veterans Affairs, BLR&D Service, to E.C.B.; and the Swedish Society for Medical Research and the Stanford Dean's Fellowship to S.N. The contents of this publication do not represent the views of the Department of Veterans Affairs or the United States government.

AUTHOR CONTRIBUTIONS

This project was funded by grants to K.K.H., E.C.B., and S.N. J.Q. designed and performed most of the experiments, in coordination with K.K.H. S.N. performed the bioinformatic analysis of the RNA-seq data. H.H.V. performed the qPCR analyses. J.Q. drafted the manuscript. K.K.H., S.N., and E.C.B. contributed to subsequent revisions.

DECLARATION OF INTERESTS

The authors declare no competing interests.

Received: February 18, 2020
Revised: August 27, 2020
Accepted: November 10, 2020
Published: December 1, 2020

REFERENCES

Afgan, E., Baker, D., Batut, B., van den Beek, M., Bouvier, D., Cech, M., Chilton, J., Clements, D., Coraor, N., Grüning, B.A., et al. (2018). The Galaxy platform for accessible, reproducible and collaborative biomedical analyses: 2018 update. Nucleic Acids Res. *46* (*W1*), W537–W544.

Alsayegh, K., Cortés-Medina, L.V., Ramos-Mandujano, G., Badraiq, H., and Li, M. (2019). Hematopoietic Differentiation of Human Pluripotent Stem Cells: HOX and GATA Transcription Factors as Master Regulators. Curr. Genomics *20*, 438–452.

Bernatchez, P.N., Soker, S., and Sirois, M.G. (1999). Vascular endothelial growth factor effect on endothelial cell proliferation, migration, and platelet-activating factor synthesis is Flk-1-dependent. J. Biol. Chem. *274*, 31047–31054.

Blankenberg, D., Gordon, A., Von Kuster, G., Coraor, N., Taylor, J., and Nekrutenko, A.; Galaxy Team (2010). Manipulation of FASTQ data with Galaxy. Bioinformatics *26*, 1783–1785.

Bohnsack, B.L., Lai, L., Dolle, P., and Hirschi, K.K. (2004). Signaling hierarchy downstream of retinoic acid that independently regulates vascular remodeling and endothelial cell proliferation. Genes Dev. *18*, 1345–1358.

Chanda, B., Ditadi, A., Iscove, N.N., and Keller, G. (2013). Retinoic acid signaling is essential for embryonic hematopoietic stem cell development. Cell *155*, 215–227.

Chao, H.X., Fakhreddin, R.I., Shimerov, H.K., Kedziora, K.M., Kumar, R.J., Perez, J., Limas, J.C., Grant, G.D., Cook, J.G., Gupta, G.P., and Purvis, J.E. (2019). Evidence that the human cell cycle is a series of uncoupled, memoryless phases. Mol. Syst. Biol. *15*, e8604.

Chetty, S., Pagliuca, F.W., Honore, C., Kweudjeu, A., Rezania, A., and Melton, D.A. (2013). A simple tool to improve pluripotent stem cell differentiation. Nat. Methods *10*, 553–556.

de Bruijn, M.F., Speck, N.A., Peeters, M.C., and Dzierzak, E. (2000). Definitive hematopoietic stem cells first develop within the major arterial regions of the mouse embryo. EMBO J. *19*, 2465–2474.

De Val, S., and Black, B.L. (2009). Transcriptional control of endothelial cell development. Dev. Cell *16*, 180–195.

Dege, C., and Sturgeon, C.M. (2017). Directed Differentiation of Primitive and Definitive Hematopoietic Progenitors from Human Pluripotent Stem Cells. J. Vis. Exp. (*129*), 55196.

Dekker, J. (2014). Two ways to fold the genome during the cell cycle: insights obtained with chromosome conformation capture. Epigenetics Chromatin *7*, 25.

Fang, J.S., Gritz, E.C., Marcelo, K.L., and Hirschi, K.K. (2016). Isolation of Murine Embryonic Hemogenic Endothelial Cells. J. Vis. Exp. (*112*), 54150.

Fang, J.S., Coon, B.G., Gillis, N., Chen, Z., Qiu, J., Chittenden, T.W., Burt, J.M., Schwartz, M.A., and Hirschi, K.K. (2017). Shear-induced Notch-Cx37-p27 axis arrests endothelial cell cycle to enable arterial specification. Nat. Commun. *8*, 2149.

Fu, X., Toh, W.S., Liu, H., Lu, K., Li, M., and Cao, T. (2011). Establishment of clinically compliant human embryonic stem cells in an autologous feeder-free system. Tissue Eng. Part C Methods *17*, 927–937.

Gao, Y., Wu, K., Chen, Y., Zhou, J., Du, C., Shi, Q., Xu, S., Jia, J., Tang, X., Li, F., et al. (2015). Beyond proliferation: KLF5 promotes angiogenesis of bladder cancer through directly regulating VEGFA transcription. Oncotarget *6*, 43791–43805.

Goldie, L.C., Lucitti, J.L., Dickinson, M.E., and Hirschi, K.K. (2008). Cell signaling directing the formation and function of hemogenic endothelium during murine embryogenesis. Blood *112*, 3194–3204.

Gonzales, K.A., Liang, H., Lim, Y.S., Chan, Y.S., Yeo, J.C., Tan, C.P., Gao, B., Le, B., Tan, Z.Y., Low, K.Y., et al. (2015). Deterministic Restriction on Pluripotent State Dissolution by Cell-Cycle Pathways. Cell *162*, 564–579.

Hitomi, M., Yang, K., Guo, Y., Fretthold, J., Harwalkar, J., and Stacey, D.W. (2006). p27Kip1 and cyclin dependent kinase 2 regulate passage through the restriction point. Cell Cycle *5*, 2281–2289.

Hosoya, T., Clifford, M., Losson, R., Tanabe, O., and Engel, J.D. (2013). TRIM28 is essential for erythroblast differentiation in the mouse. Blood *122*, 3798–3807.

Kim, D., Langmead, B., and Salzberg, S.L. (2015). HISAT: a fast spliced aligner with low memory requirements. Nat. Methods *12*, 357–360.

Krassowska, A., Gordon-Keylock, S., Samuel, K., Gilchrist, D., Dzierzak, E., Oostendorp, R., Forrester, L.M., and Ansell, J.D. (2006). Promotion of haematopoietic activity in embryonic stem cells by the aorta-gonad-mesonephros microenvironment. Exp. Cell Res. *312*, 3595–3603.

Lai, L., Bohnsack, B.L., Niederreither, K., and Hirschi, K.K. (2003). Retinoic acid regulates endothelial cell proliferation during vasculogenesis. Development *130*, 6465–6474.

Larsson, J., and Karlsson, S. (2005). The role of Smad signaling in hematopoiesis. Oncogene *24*, 5676–5692.

Lawson, N.D., Vogel, A.M., and Weinstein, B.M. (2002). Sonic hedgehog and vascular endothelial growth factor act upstream of the Notch pathway during arterial endothelial differentiation. Dev. Cell *3*, 127–136.

Lengerke, C., Grauer, M., Niebuhr, N.I., Riedt, T., Kanz, L., Park, I.H., and Daley, G.Q. (2009). Hematopoietic development from human induced pluripotent stem cells. Ann. N Y Acad. Sci. *1176*, 219–227.

Liao, Y., Smyth, G.K., and Shi, W. (2014). featureCounts: an efficient general purpose program for assigning sequence reads to genomic features. Bioinformatics *30*, 923–930.

Love, M.I., Huber, W., and Anders, S. (2014). Moderated estimation of fold change and dispersion for RNA-seq data with DESeq2. Genome Biol. *15*, 550.

Marcelo, K.L., Goldie, L.C., and Hirschi, K.K. (2013a). Regulation of endothelial cell differentiation and specification. Circ. Res. *112*, 1272–1287.

Marcelo, K.L., Sills, T.M., Coskun, S., Vasavada, H., Sanglikar, S., Goldie, L.C., and Hirschi, K.K. (2013b). Hemogenic endothelial cell specification requires c-Kit, Notch signaling, and p27-mediated cell-cycle control. Dev. Cell *27*, 504–515.

Medvinsky, A., and Dzierzak, E. (1996). Definitive hematopoiesis is autonomously initiated by the AGM region. Cell *86*, 897–906.

Melincovici, C.S., Boşca, A.B., Şuşman, S., Mărginean, M., Mihu, C., Istrate, M., Moldovan, I.M., Roman, A.L., and Mihu, C.M. (2018). Vascular endothelial growth factor (VEGF) - key factor in normal and pathological angiogenesis. Rom. J. Morphol. Embryol. *59*, 455–467.

Müller, A.M., Medvinsky, A., Strouboulis, J., Grosveld, F., and Dzierzak, E. (1994). Development of hematopoietic stem cell activity in the mouse embryo. Immunity *1*, 291–301.

Nadin, B.M., Goodell, M.A., and Hirschi, K.K. (2003). Phenotype and hematopoietic potential of side population cells throughout embryonic development. Blood *102*, 2436–2443.

Nagai, R., Suzuki, T., Aizawa, K., Shindo, T., and Manabe, I. (2005). Significance of the transcription factor KLF5 in cardiovascular remodeling. J. Thromb. Haemost. *3*, 1569–1576.

Niederreither, K., Subbarayan, V., Dollé, P., and Chambon, P. (1999). Embryonic retinoic acid synthesis is essential for early mouse post-implantation development. Nat. Genet. *21*, 444–448.

Niwa, A., Heike, T., Umeda, K., Oshima, K., Kato, I., Sakai, H., Suemori, H., Nakahata, T., and Saito, M.K. (2011). A novel serum-free monolayer culture for orderly hematopoietic differentiation of human pluripotent cells via mesodermal progenitors. PLOS ONE *6*, e22261.

Pauklin, S., and Vallier, L. (2013). The cell-cycle state of stem cells determines cell fate propensity. Cell *155*, 135–147.

Phipson, B., Lee, S., Majewski, I.J., Alexander, W.S., and Smyth, G.K. (2016). Robust Hyperparameter Estimation Protects against Hypervariable Genes and Improves Power to Detect Differential Expression. Ann. Appl. Stat. *10*, 946–963.

Poppy Roworth, A., Ghari, F., and La Thangue, N.B. (2015). To live or let die - complexity within the E2F1 pathway. Mol. Cell. Oncol. *2*, e970480.

Sakaue-Sawano, A., Kurokawa, H., Morimura, T., Hanyu, A., Hama, H., Osawa, H., Kashiwagi, S., Fukami, K., Miyata, T., Miyoshi, H., et al. (2008). Visualizing spatiotemporal dynamics of multicellular cell-cycle progression. Cell *132*, 487–498.

Sarkar, A., and Hochedlinger, K. (2013). The sox family of transcription factors: versatile regulators of stem and progenitor cell fate. Cell Stem Cell *12*, 15–30.

Schmidt, M., and Sebastian, M. (2018). Palbociclib-The First of a New Class of Cell Cycle Inhibitors. Recent Results Cancer Res. *211*, 153–175.

Singh, A.M., Chappell, J., Trost, R., Lin, L., Wang, T., Tang, J., Matlock, B.K., Weller, K.P., Wu, H., Zhao, S., et al. (2013). Cell-cycle control of developmentally regulated transcription factors accounts for heterogeneity in human pluripotent cells. Stem Cell Reports *1*, 532–544.

Sriram, G., Tan, J.Y., Islam, I., Rufaihah, A.J., and Cao, T. (2015). Efficient differentiation of human embryonic stem cells to arterial and venous endothelial cells under feeder- and serum-free conditions. Stem Cell Res. Ther. *6*, 261.

Staal, F.J., and Luis, T.C. (2010). Wnt signaling in hematopoiesis: crucial factors for self-renewal, proliferation, and cell fate decisions. J. Cell. Biochem. *109*, 844–849.

Taoudi, S., and Medvinsky, A. (2007). Functional identification of the hematopoietic stem cell niche in the ventral domain of the embryonic dorsal aorta. Proc. Natl. Acad. Sci. USA *104*, 9399–9403.

Tumbar, T., and Belmont, A.S. (2001). Interphase movements of a DNA chromosome region modulated by VP16 transcriptional activator. Nat. Cell Biol. *3*, 134–139.

Wulf, G.G., Luo, K.L., Jackson, K.A., Brenner, M.K., and Goodell, M.A. (2003). Cells of the hepatic side population contribute to liver regeneration and can be replenished with bone marrow stem cells. Haematologica *88*, 368–378.

STAR★METHODS

KEY RESOURCES TABLE

REAGENT or RESOURCE	SOURCE	IDENTIFIER
Antibodies		
Pacific Blue anti-human CD31 Antibody	BioLegend	Cat#303113; RRID:AB_1877196
FITC anti-human CD31 Antibody	BioLegend	Cat#303104; RRID:AB_314330
Alexa Fluor® 700 anti-human CD45 Antibody	BioLegend	Cat#304024; RRID:AB_493761
APC/Cyanine7 anti-human CD45 Antibody	BioLegend	Cat#304014; RRID:AB_314402
PE/Cy7 anti-human CD309 (VEGFR2) Antibody	BioLegend	Cat#359911; RRID:AB_2563551
APC anti-human CD117 (c-kit) Antibody	BioLegend	Cat#313206; RRID:AB_314985
PE anti-human CD144 (VE-Cadherin) Antibody	BioLegend	Cat#348506; RRID:AB_2077978
Pacific Blue anti-human CD34 Antibody	BioLegend	Cat#343512; RRID:AB_1877197
FITC anti-human CD20 Antibody	BioLegend	Cat#302303; RRID:AB_314251
Brilliant Violet 421 anti-human CD3 Antibody	BioLegend	Cat#317343; RRID:AB_2565848
Brilliant Violet 421 anti-human CD14 Antibody	BioLegend	Cat#325627; RRID:AB_2561342
Alexa Fluor® 594 anti-human CD66b Antibody	BioLegend	Cat#392907
Alexa Fluor® 488 anti-human CD41 Antibody	BioLegend	Cat#303723; RRID:AB_2566302
APC anti-human CD235ab Antibody	BioLegend	Cat#306607; RRID:AB_314625
PE anti-human CD11b Antibody	BioLegend	Cat#301305; RRID:AB_314157
Alexa Fluor® 700 anti-human CD45 Antibody	BioLegend	Cat#304024; RRID:AB_493761
Zombie NIR Fixable Viability Kit	BioLegend	Cat#423105
Chemicals, Peptides, and Recombinant Proteins		
Stemolecule CHIR99021	Stemgent	Cat#04-0004
Recombinant Human FGF basic/FGF2/ bFGF (146 aa) Protein	R&D systems	Cat#233-FB-025
Recombinant Human BMP-4 Protein	R&D systems	Cat#314-BP-010
Recombinant Human VEGF165	PeproTech	Cat#100-20
Retinoic acid	Sigma-Aldrich	Cat#R2625-50MG
AGN 194310	MedChemExpress	Cat#HY-16681
PD 0332991 isethionate	Sigma-Aldrich	Cat#PZ0199-5MG
CVT-313	Santa Cruz Biotechnology	Cat#199986-75-9
Giemsa stain, modified	Sigma-Aldrich	Cat#GS500-500ml
Normocin - Antimicrobial Reagent	InvivoGen	Cat#ant-nr-1
Fibronectin Human Protein, Plasma	GIBCO	Cat#33016015
Corning® Matrigel® Growth Factor Reduced (GFR) Basement Membrane Matrix, LDEV-free, 5 mL	Corning	Cat#356230
Critical Commercial Assays		
RNeasy Plus Micro Kit	QIAGEN	Cat#74034
5X All-In-One RT MasterMix	abm	Cat#G490
miScript SYBR® Green PCR Kit	QIAGEN	Cat#218073

(*Continued on next page*)

Continued

REAGENT or RESOURCE	SOURCE	IDENTIFIER
DiI-Ac-LDL Kit	Cell Applications	Cat#022K
Deposited Data		
RNA-seq-1	This paper	GSE159694
RNA-seq-2	This paper	GSE159694
Experimental Models: Cell Lines		
H1-hESC	Yale Stem Cell Center	N/A
H9-Fucci-hESC	Pauklin and Vallier, 2013	N/A
Experimental Models: Organisms/Strains		
Mouse: B6.Cg-Tg(FucciG1)#596Bsi	Riken	Cat#RBRC02707
Mouse: C57BL/6J	JAX	Cat#000664
Oligonucleotides		
See Table S1 for oligonucleotide sequences	N/A	N/A
Software and Algorithms		
Prism 7	Graphpad Software	https://www.graphpad.com/scientific-software/prism/
ImageJ	NIH	https://imagej.nih.gov/ij/
bcl2fastq2_v2.19.0	Illumina	https://support.illumina.com/sequencing/sequencing_software/bcl2fastq-conversion-software.html
Galaxy	Afgan et al., 2018	https://usegalaxy.org/
DESeq2	Love et al., 2014	N/A
ComplexHeatmap	Phipson et al., 2016	N/A
limma	Phipson et al., 2016	N/A

RESOURCE AVAILABILITY

Lead Contact

Further information and requests for resources and reagents should be directed to and will be fulfilled by the Lead Contact, Karen K. Hirschi (kkh4yy@virginia.edu).

Materials Availability

This study did not generate new unique reagents.

Data and Code Availability

The accession number for the RNA-seq data reported in this paper is Gene Expression Omnibus (GEO): GSE159694.

EXPERIMENTAL MODEL AND SUBJECT DETAILS

Cell culture

H1-hESC were obtained from Yale Stem Cell Center and used up to passage 90. H9-Fucci-hESC were obtained from Dr. Ludovic Vallier's lab at Cambridge Stem Cell Institute and used up to passage 90 (Pauklin and Vallier, 2013). All hESC were cultured in mTeSR™ medium (STEMCELL Technologies cat# 85850) on Matrigel-coated plates (Corning® Matrigel® Growth Factor Reduced (GFR) Basement Membrane Matrix, LDEV-free, 5 mL, Corning cat# 356230) as described in Fu et al. (2011). Importantly, 50 μg/ml G-418 solution (Sigma cat# 4727878001) was added to the culture medium for H9-Fucci-hESC to eliminate non-transduced cells. For passage, 160 μl/ml Dispase (STEMCELL Technologies cat# 07913) was added to cell culture. Cells were incubated with Dispase at 37°C for 45min. Afterward, cells were transferred to Falcon tubes containing DMEM:F12 medium (GIBCO cat# 11320-033) for washing. 12ml of DMEM:F12 medium was used per 1ml of cell culture medium. Let tubes stand at room temperature for 5-10min or until all cell pellets settle to the bottom of the tubes. Remove supernatant and cells were resuspended in mTeSR™ medium, dispersed into small clumps, and re-plated onto Matrigel-coated plates.

Animals

All animals used were on a C57BL/6 background (female, 8 – 12 weeks old) and all studies were conducted in compliance with Yale's Institutional Animal Care and Usage Committee guidelines. FUCCI-red animals (B6.Cg-Tg(FucciG1)#596Bsi, Riken, cat# RBRC02707) were crossed with either FUCCI-red animals or wild-type C57BL/6J animals (JAX, cat# 000664).

METHOD DETAILS

Differentiation protocol

H1-hESC or H9-Fucci-hESC were passaged using the method described above and re-plated onto Matrigel-coated plates. These hESC colonies were maintained in mTeSR for 24 hours, after which the cells were gently washed with DMEM:F12 and differentiated in chemically defined, serum-free, animal component-free medium STEMdiffAPEL2 (STEMCELL Technologies cat# 05270) supplemented with Protein-Free Hybridoma Medium (PFHM-II, GIBCO, cat# 12040077) by adding 5 mL of PFHM to 100 mL of STEMdiffAPEL2 medium. Growth factors depicted in Figure 1A were added sequentially (Stemolecule CHIR99021, 5 μM, Stemgent cat# 04-0004; Recombinant Human FGF basic/FGF2/bFGF (146 aa) Protein, 50 ng/ml, R&D systems cat# 233-FB-025; Recombinant Human BMP-4 Protein, 25 ng/ml, R&D systems cat# 314-BP-010; Recombinant Human VEGF165, 50 ng/ml, PeproTech, cat# 100-20) as described in Sriram et al. (2015). For certain experiments, cells were treated with RA (0.5 μM, Sigma-Aldrich, cat# R2625-50MG), RAi (AGN 194310, 6nM, MedChemExpress, cat# HY-16681), CDK4/6i (PD 0332991 isethionate, 2nM, Sigma-Aldrich, cat# PZ0199-5MG), and/or CDK2i (CVT-313, 0.5 μM, Santa Cruz Biotechnology, cat# 199986-75-9) every 24hrs starting Day5.

qPCR

Transcriptomes were prepared from cultured hESC/hESC-derived cells using RNeasy Plus Micro Kit (QIAGEN, cat# 74034) and 5X All-In-One RT MasterMix (abm, cat# G490). Resulting cDNA libraries were probed by qPCR using published qPCR primers (PrimerBank, sequences listed in Table S1) and miScript SYBR® Green PCR Kit (QIAGEN, cat# 218073).

Giemsa stain

1ml of supernatant was taken on Day8 of differentiation and dispersed onto a microscope slide using a slide centrifuge. Slides were then fixed in methanol for 5min. Upon air drying the slides, Giemsa Stain (Sigma-Aldrich, cat# GS500-500ml) was diluted 1:20 with deionized water and slides were stained for 60min at room temperature. Afterward slides were briefly rinsed with deionized water, air-dried, and mounted to be evaluated under a microscope.

Flow cytometry analysis for cell culture

Buffer list: sorting buffer (HBSS, GIBCO, cat# 14175-095; 1%FBS, Gemini Bio, cat# 100-106; supplemented with 1:500 diluted Normocin - Antimicrobial Reagent, InvivoGen, cat# ant-nr-1); antibody staining buffer (HBSS; 10%FBS; supplemented with 1:500 diluted Normocin); Hoechst staining buffer (DMEM:F12-high glucose, GIBCO, cat# 11965-092; 10%FBS; supplemented with 1:500 diluted Normocin).

Antibody list: Pacific Blue anti-human CD31 Antibody (BioLegend, cat# 303113), FITC anti-human CD31 Antibody (BioLegend, cat# 303104), Alexa Fluor® 700 anti-human CD45 Antibody (BioLegend, cat# 304024), APC/Cyanine7 anti-human CD45 Antibody (BioLegend, cat# 304014), PE/Cy7 anti-human CD309 (VEGFR2) Antibody (BioLegend, cat# 359911), APC anti-human CD117 (c-kit) Antibody (BioLegend, cat# 313206), PE anti-human CD144 (VE-Cadherin) Antibody (BioLegend, cat# 348506), Pacific Blue anti-human CD34 Antibody (BioLegend, cat# 343512), FITC anti-human CD20 Antibody (BioLegend, cat# 302303), Brilliant Violet 421 anti-human CD3 Antibody (BioLegend, cat# 317343), Brilliant Violet 421 anti-human CD14 Antibody (BioLegend, cat# 325627), Alexa Fluor® 594 anti-human CD66b Antibody (BioLegend, cat# 392907), Alexa Fluor® 488 anti-human CD41 Antibody (BioLegend, cat# 303723), APC anti-human CD235ab Antibody (BioLegend, cat# 306607), PE anti-human CD11b Antibody (BioLegend, cat# 301305), Alexa Fluor® 700 anti-human CD45 Antibody (BioLegend, cat# 304024), Zombie NIR Fixable Viability Kit (BioLegend, cat# 423105).

If side population staining was needed, prewarmed Hoechst staining buffer in 37°C water bath for 15min. Differentiated cells were harvested with Accutase (STEMCELL Technologies, cat# 7920) and spun 5min at 1,000x*rcf.* at 4°C to pellet. Cells were then washed once with DMEM:F12 and spun 5min at 1,000x*rcf.* at 4°C to pellet. Cells were resuspended in prewarmed Hoechst staining buffer such that cells were at a final concentration of $1x10^6$ cells/ml. At least 100 μL of sample ($1x10^5$ cells) was aliquoted into fresh 1.5 mL tubes for control. The following sample and necessary control tubes were included: Unstained; Hoechst 33342 only; Hoechst 33342 only + Verapamil; all single-color antibody controls; Sample (received all colors, except for Verapamil). Verapamil diluted in 95% ethanol was added to the "Hoechst 33342 only + Verapamil" control tube to a final concentration of 50 μM. All tubes were incubated for 5 minutes at 37°C. (CAUTION: Verapamil is a potent calcium-channel blocking agent and is extremely toxic. Handle with gloves). Hoechst 33342 was then added to the "Hoechst 33342 only" control, to the Hoechst 33342 + Verapamil only control, and to the "Sample" tube to a final concentration of 5 μg/ml. All tubes were incubated for 1 hour at 37°C, protected from light. Tubes were gently mixed through inversion every 15 minutes. (CAUTION: Hoechst 33342 is a toxic nuclear dye and should be handled with gloves). Tubes were spun 5min at 1,000x*rcf.* at 4°C to pellet. Supernatant was removed and cell pellets were resuspended at a concentration of $1x10^5$ cells/ml in cold antibody staining buffer. Fluorescently-conjugated antibodies were added to appropriate

antibody-only control tubes, and to the "Sample" tube. Dilutions need to be optimized for different antibodies and FACS machines. Tubes were incubated on ice for 30 minutes, protected from light. Afterward tubes were spun 5min at 1,000x*cf.* at 4°C to pellet. Supernatant was removed and cell pellets were resuspended in 600 μL ice-cold sorting buffer. Samples were strained through mesh filter cap of 5 mL round bottom polystyrene FACS tube (Corning, cat# 352235) and stored on ice, protected from light, for immediate FACS.

Methylcellulose-based blood forming assay

For population level assay, cells were sorted using FACS and seeded onto fibronectin coated dishes (Fibronectin Human Protein, Plasma, 4 μg/cm^2, GIBCO, cat# 33016015) as described in Dege and Sturgeon (2017), with MethoCult H4435 Enriched (STEMCELL Technologies, cat# 4435). For single-cell level assay, cells were directly sorted into fibronectin coated 96-well plates using FACS. Afterward, a P1000 tip with the tip trimmed to widen its bore was used to gently resuspend each well of the seeded methylcellulose media in a tissue culture hood to ensure optimal growth.

CFU-E erythroid colony and BFU-E erythroid colony were analyzed 8 days after plating. CFU-GM granulocyte-monocyte colony and CFU-GEMM multipotent hematopoietic progenitor colony were analyzed 14 days after plating.

DiI AcLDL uptake

To demonstrate endothelial phenotypic function of hESC-derived hemogenic endothelial cells in culture, active uptake of DiI AcLDL was measured. On Day3 of culturing of hESC-derived hemogenic endothelial cells in MethoCult H4435 Enriched medium (STEMCELL Technologies, cat# 4435), medium was removed and cells were washed 3 times with 1xPBS (GIBCO, cat# 10010031) to remove the residual methylcellulose medium. 1ml of endothelial cell medium (PromoCell, cat# C-22011) was added to the dish and cells were stained with 10 μg/ml DiI AcLDL (DiI-Ac-LDL Kit, Cell Applications, cat# 022K) for 4hrs at 37°C and then imaging with fluorescence microscope.

Immunostaining of hematopoietic colonies

Antibody list: Alexa Fluor® 488 anti-human CD41 Antibody (Biolegend, cat# 303723), APC anti-human CD235ab Antibody (Biolegend, cat# 306607), CD66b-Alexa594 (Biolegend, cat# 392907), CD14-BV421 (Biolegend, cat# 325627).

Single hemogenic endothelial cell was seeded in fibronectin coated 96-well plates (Cellvis, cat# P96-1.5P) as described above. Cells were cultured in 100 μL of methylcellulose medium (STEMCELL Technologies, cat# 4435) per well for 8 days before staining for CFU-E and BFU-E, for 14 days before staining for CFU-GM and CFU-GEMM. For staining, antibodies were 1:100 diluted in IMDM (GIBCO, cat# 12440046). 30 μL of diluted antibodies was added to each well on top of the methylcellulose medium (pipette slowly so as not to disturb the hematopoietic colonies). Incubate plates at 37°C overnight before imaging with fluorescence microscope.

Flow cytometry analysis for animal tissue

Flow cytometry was performed as described in Fang et al. (2016). The list of antibodies used can also be found in Fang et al. (2016).

QUANTIFICATION AND STATISTICAL ANALYSIS

RNA sequencing

All mRNA samples were isolated using RNeasy Plus Micro Kit (QIAGEN, cat# 74034). Next-generation whole transcriptome Illumina sequencing was performed with the Yale Center for Genome Analysis. Fastq-files were generated with bcl2fastq2_v2.19.0 and then uploaded to the usegalaxy.org platform (Afgan et al., 2018) for quality control and trimming (Galaxy ToolShed v 1.0.2; FASTQ/A short-reads pre-processing tools: http://hannonlab.cshl.edu/fastx_toolkit/) (Blankenberg et al., 2010). Sequences were aligned to the hg38 genome using HISAT2 (v 2.1.0+galaxy4) (Kim et al., 2015) and aligned sequences were quantified with featureCounts (v 1.6.3+galaxy2) (Liao et al., 2014). Differential gene expression analysis was performed with DESeq2 (R package v 1.24.0) (Love et al., 2014) using unmanipulated count data. Heatmaps were generated with ComplexHeatmap (R package v 2.0.0) using data transformed with DESeq2 and batch-corrected with limma (R package v 3.40.6) (Phipson et al., 2016).

Statistical analysis

Two-tailed Student's t tests were performed using Prism 7 for MacOSX software

for all analyses. p values < 0.05 were considered as significant: *, $p \leq 0.05$; **, $p \leq 0.01$; ***, $p \leq 0.001$; ****, $p \leq 0.0001$. Standard deviations are depicted in all graphs.

Cell Reports, Volume *33*

Supplemental Information

Retinoic Acid Promotes Endothelial Cell Cycle Early G1 State to Enable Human Hemogenic Endothelial Cell Specification

Jingyao Qiu, Sofia Nordling, Hema H. Vasavada, Eugene C. Butcher, and Karen K. Hirschi

Supplemental Information

Supplementary Table 1

CDH5-F	GCAGCAGCAGGTGCTAACC
CDH5-R	TTGCCCACATATTCTCCTTTG
EFNB2-F	TATGCAGAACTGCGATTTCCAA
EFNB2-R	TGGGTATAGTACCAGTCCTTGTC
EPHB4-F	TGAAGAGGTGATTGGTGCAG
EPHB4-R	AGGCCTCGCTCAGAAACTCAC
GAPDH-F	ACAACTTTGGTATCGTGGAAGG
GAPDH-R	GCCATCACGCCACAGTTTC
HAND1-F	GAGAGCATTAACAGCGCATTCG
HAND1-R	CGCAGAGTCTTGATCTTGGAGAG
RUNX1-F	TGAGCTGAGAAATGCTACCGC
RUNX1-R	ACTTCGACCGACAAACCTGAG
SOX2-F	GCCGAGTGGAAACTTTTGTCG
SOX2-R	GGCAGCGTGTACTTATCCTTCT
TBXT-F	TATGAGCCTCGAATCCACATAGT
TBXT-R	CCTCGTTCTGATAAGCAGTCAC

Supplementary Table 1: Sequences of primers used for qPCR. Related to Figure 1.
All sequences are listed in 5’ to 3’ orientation.

Supplementary Figure 1

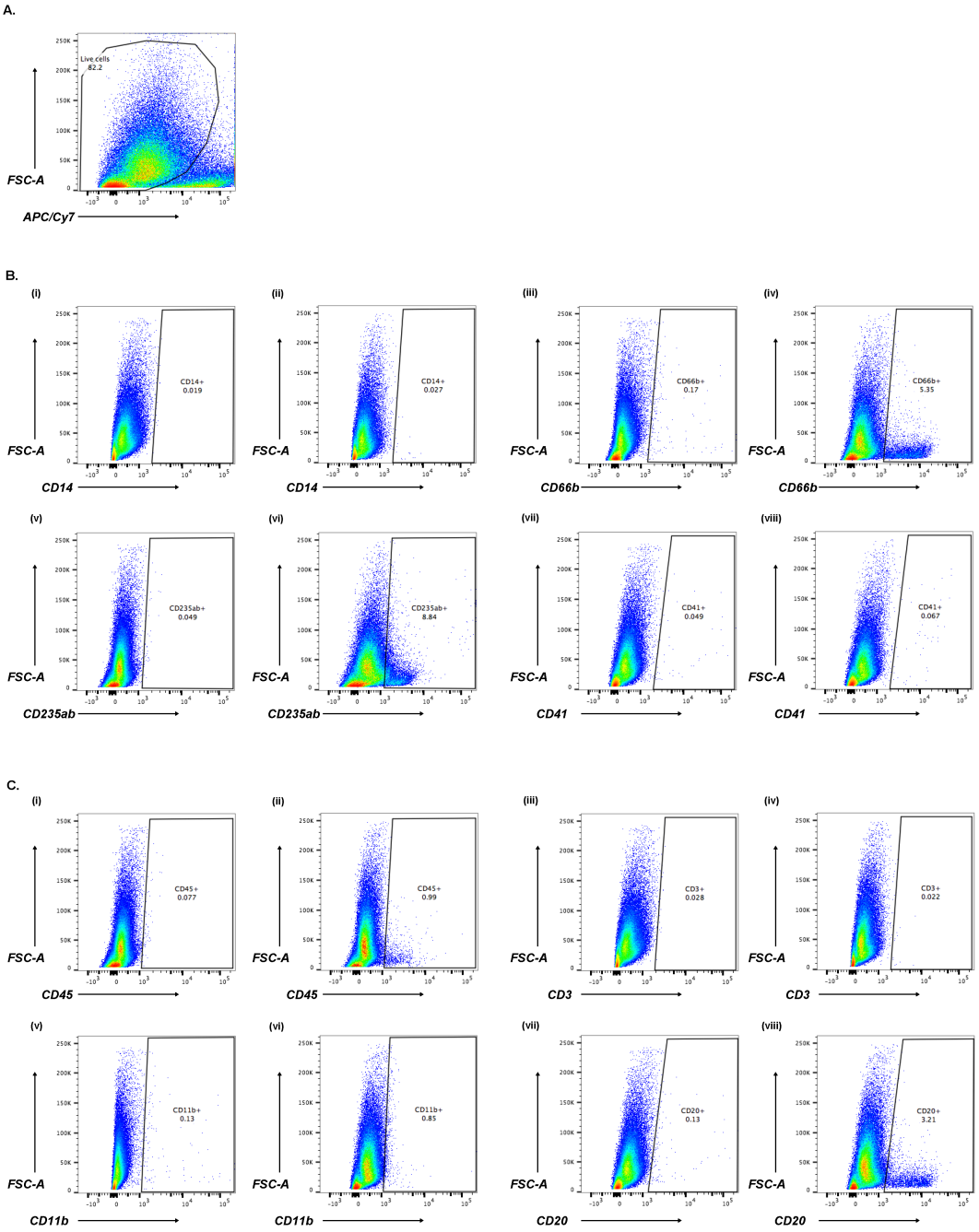

Supplementary Figure 1: Blood cells of multiple lineages were identified within adherent cell population on Day8 of differentiation. Related to Figure 1. Expression of various blood cell markers were evaluated on Day8 of differentiation for adherent cells. Flow cytometry analyses were done using two panels of markers. n=3 for all groups. A) Live vs. dead cells were distinguished using a viability dye that is non-permeable to live cells. B) Expression of blood cell markers within the adherent cell population (panel 1). (i)

Expression of CD14 in adherent cells (unstained control). (ii) Expression of CD14 in adherent cells. (iii) Expression of CD66b in adherent cells (unstained control). (iv) Expression of CD66b in adherent cells. (v) Expression of CD235ab in adherent cells (unstained control). (vi) Expression of CD235ab in adherent cells. (vii) Expression of CD41 in adherent cells (unstained control). (viii) Expression of CD41 in adherent cells. C) Expression of blood cell markers within the adherent cell population (panel 2). (i) Expression of CD45 in adherent cells (unstained control). (ii) Expression of CD45 in adherent cells. (iii) Expression of CD3 in adherent cells (unstained control). (iv) Expression of CD3 in adherent cells. (v) Expression of CD11b in adherent cells (unstained control). (vi) Expression of CD11b in adherent cells. (vii) Expression of CD20 in adherent cells (unstained control). (viii) Expression of CD20 in adherent cells.

Supplementary Figure 2

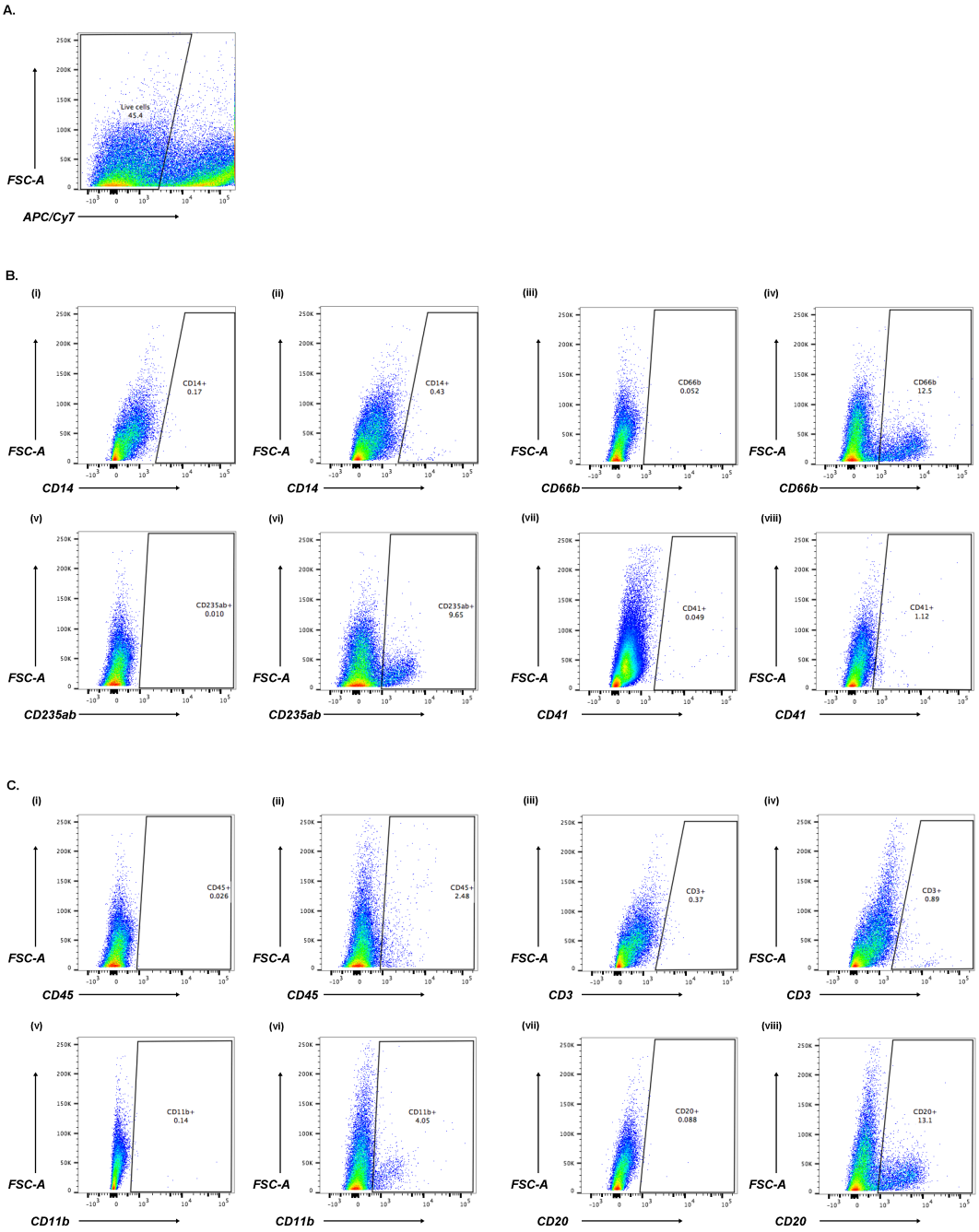

Supplementary Figure 2: Blood cells of multiple lineages were identified within suspended cell population on Day8 of differentiation. Related to Figure 1. Expression of various blood cell markers were evaluated on Day8 of differentiation for suspended cells. Flow cytometry analyses were done using two panels of markers. n=3 for all groups. A) Live vs. dead cells were distinguished using a viability dye that is non-permeable to live cells. B) Expression of blood cell markers within the suspended cell

population (panel 1). (i) Expression of CD14 in suspended cells (unstained control). (ii) Expression of CD14 in suspended cells. (iii) Expression of CD66b in suspended cells (unstained control). (iv) Expression of CD66b in suspended cells. (v) Expression of CD235ab in suspended cells (unstained control). (vi) Expression of CD235ab in suspended cells. (vii) Expression of CD41 in suspended cells (unstained control). (viii) Expression of CD41 in suspended cells. C) Expression of blood cell markers within the suspended cell population (panel 2). (i) Expression of CD45 in suspended cells (unstained control). (ii) Expression of CD45 in suspended cells. (iii) Expression of CD3 in suspended cells (unstained control). (iv) Expression of CD3 in suspended cells. (v) Expression of CD11b in suspended cells (unstained control). (vi) Expression of CD11b in suspended cells. (vii) Expression of CD20 in suspended cells (unstained control). (viii) Expression of CD20 in suspended cells.

Supplementary Figure 3

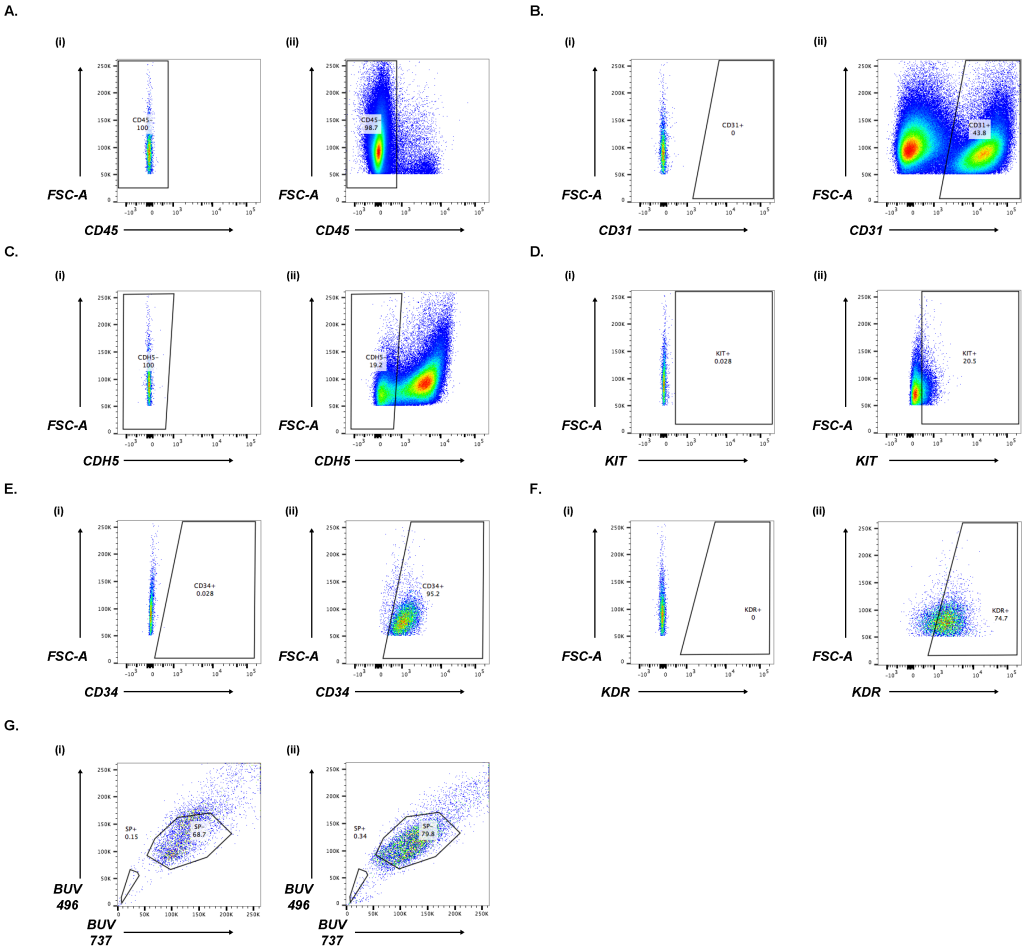

H.

Surface Marker	Percentage of Total Cells (%)	Cumulative Fold-Enrichment for Hemogenic Endothelial Cells
CD45-	98.7	-
CD31+CD45-	43.2	2.3
CD31+CDH5-CD45-	8.3	11.9
CD31+KIT+CDH5-CD45-	1.7	58.1
CD31+KIT+CD34+CDH5-CD45-	1.6	61.7
CD31+KDR+KIT+CD34+CDH5-CD45-	1.2	82.3

Supplementary Figure 3: Characterizing the phenotype of human hemogenic endothelial cells. Related to Figure 2. Expression of various potential markers of human hemogenic endothelial cells were evaluated by flow cytometry on Day8 of differentiation. A) Expression of CD45 within all cultured cells. (i) Unstained control. (ii) Sample. B) Expression of CD31 within CD45- cells. (i) Unstained control. (ii) Sample. C) Expression of CDH5 within CD31+CD45- cells. (i) Unstained control. (ii) Sample. D) Expression of KIT within CD31+CD45-CDH5- cells. (i) Unstained control. (ii) Sample. E) Expression of CD34 within CD31+CD45-CDH5-KIT+ cells. (i) Unstained control. (ii) Sample. F) Expression of KDR within CD31+CD45-CDH5-KIT+CD34+ cells. (i) Unstained control. (ii) Sample. G) Expression of SP within CD31+CD45-CDH5-KIT+CD34+ cells.

SP events were identified using a differential linear-scale plot of Hoechst blue (BUV 496) vs. Hoechst red (BUV 737) fluorescence. (i) Verapamil control. (ii) Sample. H) Enrichment of CD31+KDR+KIT+CD34+CDH5-CD45- hemogenic endothelial cells is shown in the table. Cumulative fold-enrichment for hemogenic endothelial cells was calculated by comparing each group to the original CD45- group.

Supplementary Figure 4

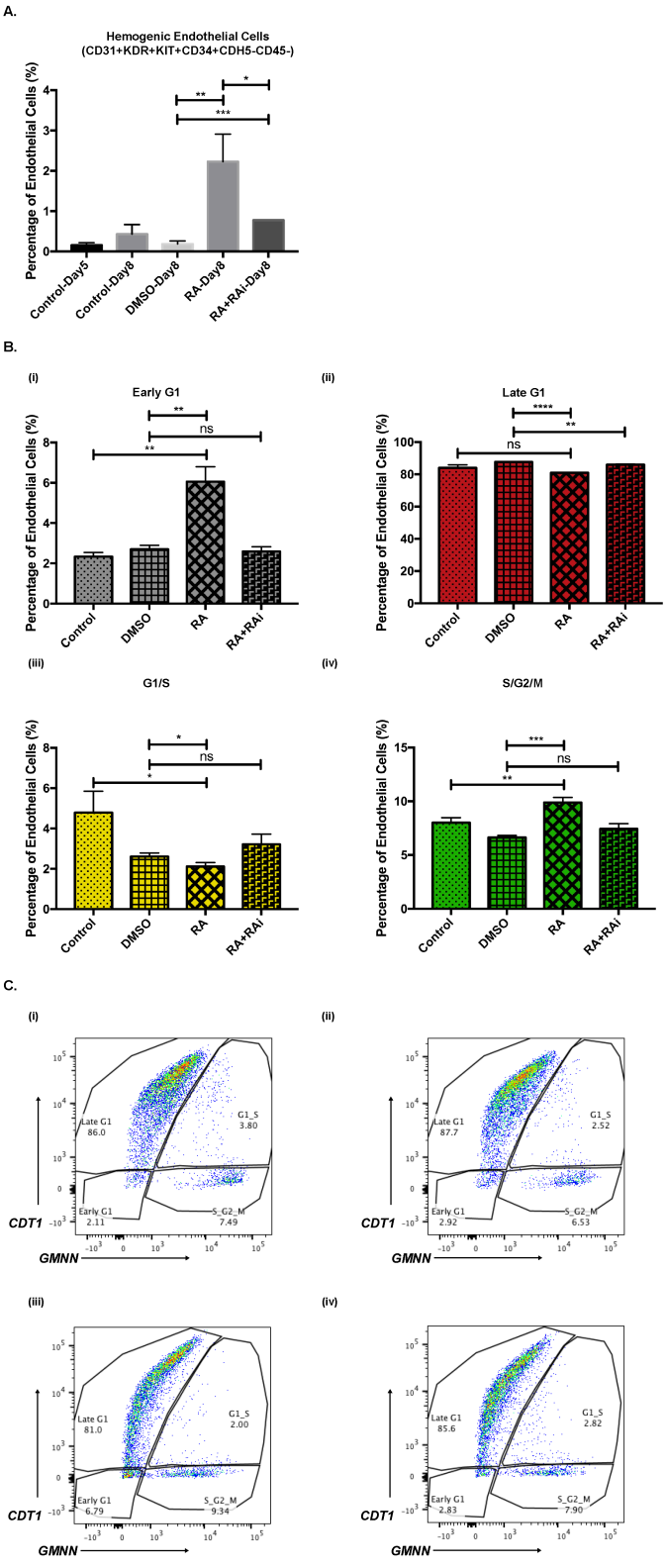

Supplementary Figure 4: RA promotes early G1 cell cycle state of hESC-derived endothelial cells and their specification toward hemogenic endothelial cells (percentage shown). Related to Figure 4. A) RA induces differentiation of hemogenic endothelial cells. n=3 for all groups. Students' t-test: $p = 0.0068$ (DMSO vs. RA), $p = 0.0005$ (DMSO vs. RA+RAi), $p = 0.0218$ (RA vs. RA+RAi). B) RA induces early G1 cell cycle enrichment in endothelial cells. Cell cycle distribution was measured by expression of the FUCCI reporter construct using flow cytometry. n=3 for all groups. (i) Students' t-test: $p = 0.0011$ (control vs. RA), $p = 0.0016$ (DMSO vs. RA). (ii) Students' t-test: $p < 0.0001$ (DMSO vs. RA), $p = 0.0026$ (DMSO vs. RA+RAi). (iii) Students' t-test: $p = 0.0127$ (control vs. RA), $p = 0.0311$ (DMSO vs. RA). (iv) Students' t-test: $p = 0.0084$ (control vs. RA), $p = 0.0004$ (DMSO vs. RA). C) Representative flow cytometry dot plot of endothelial cell cycle distribution on Day 8 upon treatment of (i) control on Day5. (ii) DMSO on Day5. (iii) RA on Day5. (iv)RA+RAi on Day5.

Supplementary Figure 5

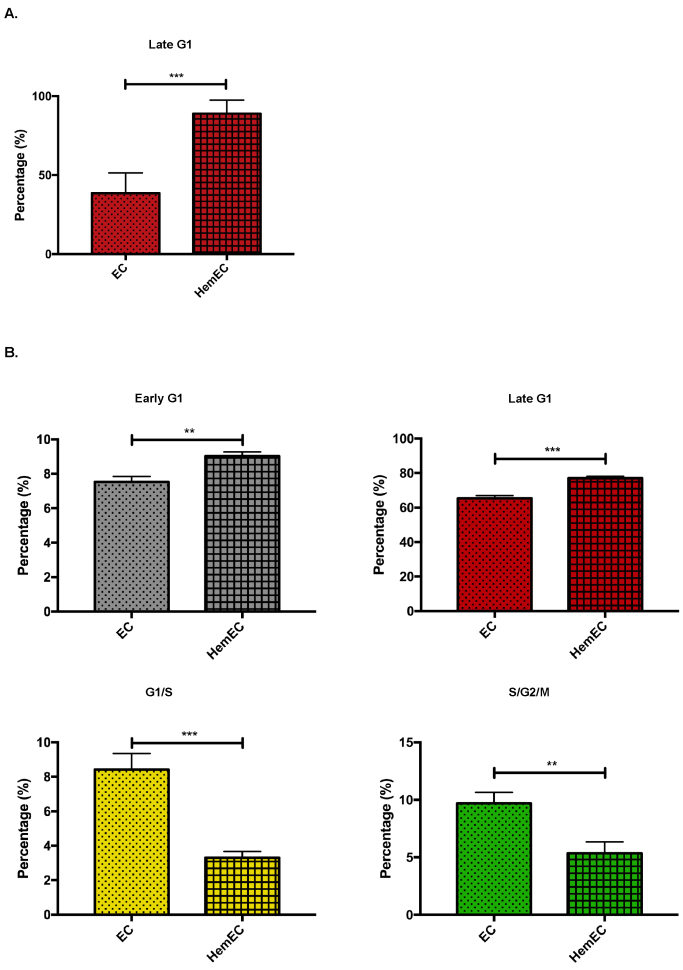

Supplementary Figure 5: Mouse and human hemogenic endothelial cells are predominantly in G1 cell cycle state in vivo and in vitro. Related to Figure 4. A) In E10.5 mouse AGM, significantly more hemogenic endothelial cells were in late G1 phase compared to non-blood forming endothelial cells. n=4 for all groups. Students' t-test: p = 0.0006. B) In hESC culture on Day8, significantly more hemogenic endothelial cells were in early and late G1 compared to non-blood-forming endothelial cells. n=3 for all groups. Students' t-test: p = 0.0031 (Early G1), p = 0.0005 (Late G1), p = 0.0009 (G1/S), p = 0.0054 (S/G2/M).

Supplementary Figure 6

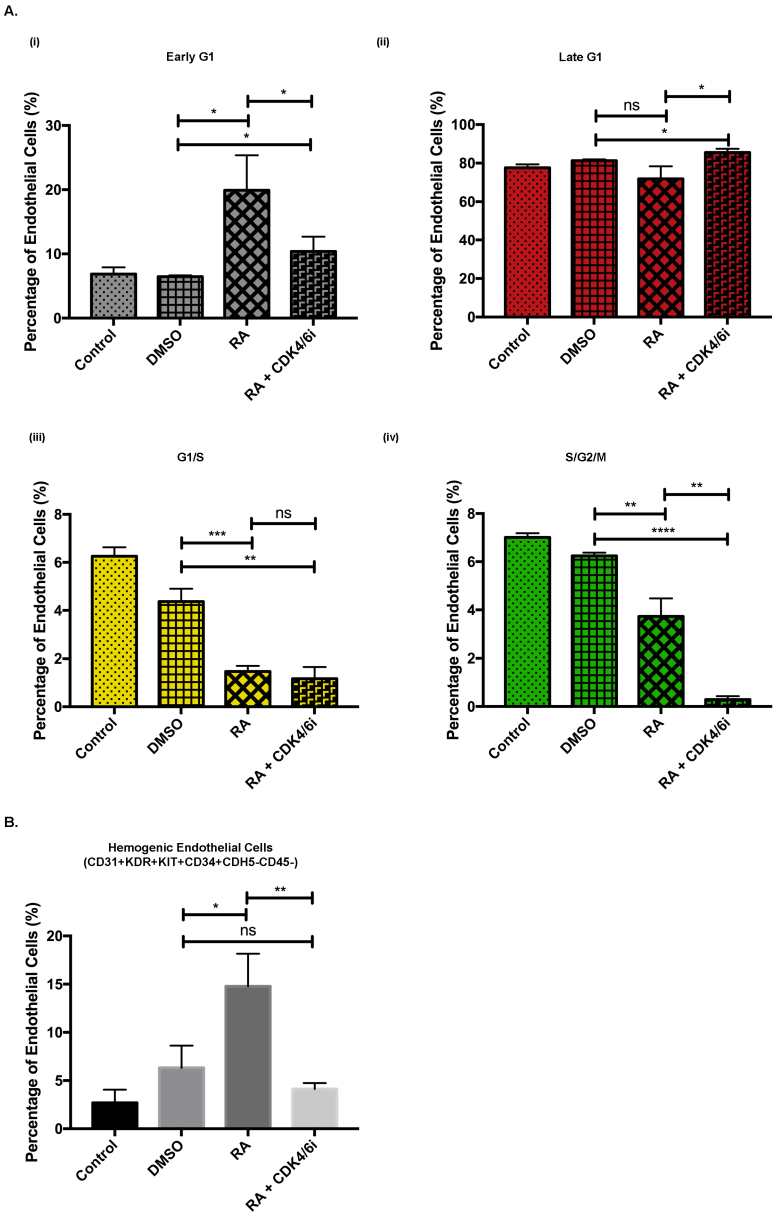

Supplementary Figure 6: Early G1 cell cycle state of endothelial cells is necessary to enable hemogenic specification (percentage shown). Related to Figure 5. A) When cells were treated with both RA and CDK4/6i, CDK4/6i overrides RA's effect on cell cycle state and enriches endothelial cells in late G1 phase. Cell cycle distribution was measured by expression of the FUCCI reporter construct using flow cytometry. n=3 for all groups. (i) Students' t-test: p = 0.0130 (DMSO vs. RA), p = 0.0423 (DMSO vs. RA+CDK4/6i), p = 0.0497 (RA vs. RA+CDK4/6i). (ii) Students' t-test: p = 0.0205 (DMSO vs. RA+CDK4/6i), p = 0.0253 (RA vs. RA+CDK4/6i). (iii) Students' t-test: p = 0.0010 (DMSO vs. RA), p = 0.0016 (DMSO vs. RA+CDK4/6i). (iv) Students' t-test: p = 0.0046

(DMSO vs. RA), $p < 0.0001$ (DMSO vs. RA+CDK4/6i), $p = 0.0015$ (RA vs. RA+CDK4/6i). B) In the absence of early G1 cell cycle arrest in endothelial cells, RA + CDK4/6i could not induce hemogenic endothelial cell specification. n=3 for all groups. Students' t-test: $p = 0.0233$ (DMSO vs. RA), $p = 0.0059$ (RA vs. RA+CDK4/6i).

Supplementary Figure 7

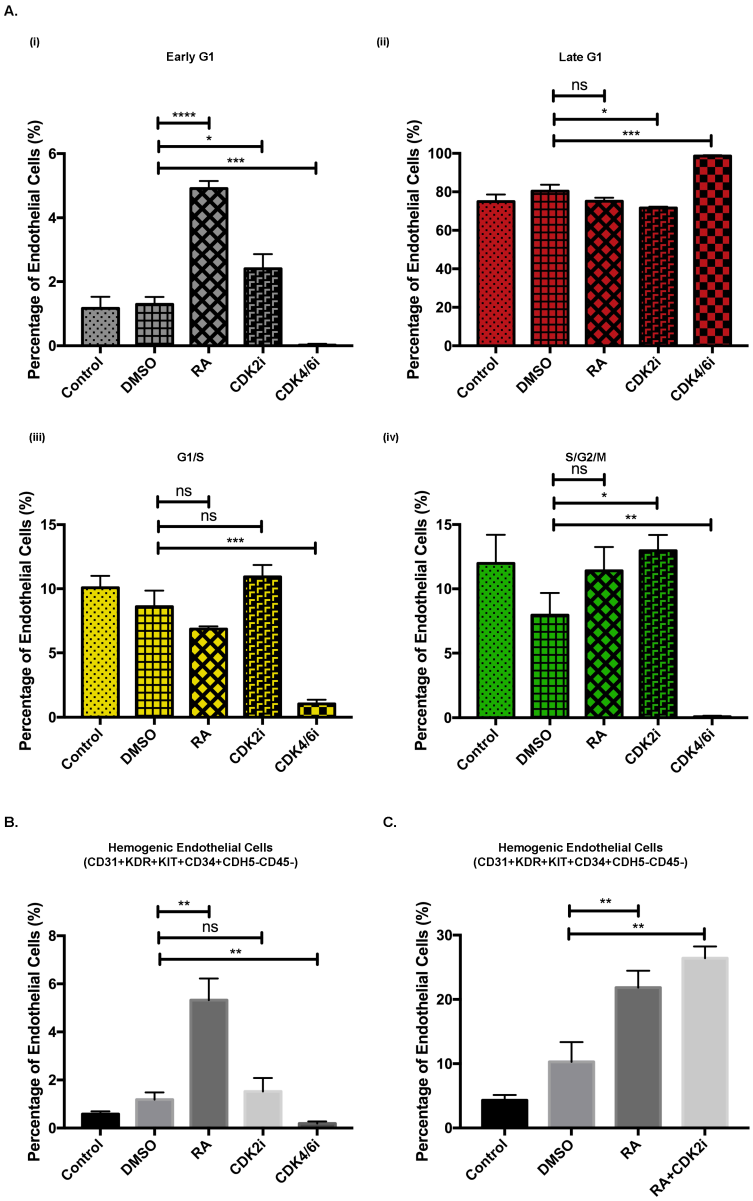

Supplementary Figure 7: Early G1 cell cycle state of endothelial cells is not sufficient, to enable hemogenic specification (percentage shown). Related to Figure 5. A) Similar to RA, CDK2i induces early G1 cell cycle arrest in endothelial cells. Cell cycle distribution was measured by expression of the FUCCI reporter construct using flow cytometry. n=3 for all groups. (i) Students' t-test: $p < 0.0001$ (DMSO vs. RA), $p = 0.0196$ (DMSO vs. CDK2i), $p = 0.0007$ (DMSO vs. CDK4/6i). (ii) Students' t-test: $p = 0.0115$ (DMSO vs. CDK2i), $p = 0.0007$ (DMSO vs. CDK4/6i). (iii) Students' t-test: $p = 0.0005$ (DMSO vs. CDK4/6i). (iv) Students' t-test: $p = 0.0148$ (DMSO vs. CDK2i), $p = 0.0014$ (DMSO vs. CDK4/6i). B) Unlike RA, CDK2i could not induce hemogenic

endothelial cell specification. n=3 for all groups. Students' t-test: p = 0.0016 (DMSO vs. RA), p = 0.0051 (DMSO vs. CDK4/6i). C) CDK2i did not artificially suppress cell growth or cell differentiation in culture. Students' t-test: p = 0.0077 (DMSO vs. RA), p = 0.0015 (DMSO vs. RA+CDK2i).